MAJOR ARTICLE

Inhibition of the Injectisome and Flagellar Type III Secretion Systems by INP1855 Impairs *Pseudomonas aeruginosa* Pathogenicity and Inflammasome Activation

Ahalieyah Anantharajah,[1] Emmanuel Faure,[2] Julien M. Buyck,[1,a] Charlotta Sundin,[3,a] Tuulikki Lindmark,[3,a] Joan Mecsas,[4] Timothy L. Yahr,[5] Paul M. Tulkens,[1] Marie-Paule Mingeot-Leclercq,[1] Benoît Guery,[2] and Françoise Van Bambeke[1]

[1]Pharmacologie cellulaire et moléculaire, Louvain Drug Research Institute, Université catholique de Louvain, Brussels, Belgium; [2]EA7366, Host-Pathogen Translational Research Group, Faculté de Médecine, Université Lille Nord de France, Lille, France; [3]Creative Antibiotics, Umeå, Sweden; [4]Department of Molecular Biology and Microbiology, Tufts University School of Medicine, Boston, Massachusetts; and [5]Department of Microbiology, University of Iowa, Iowa City

With the rise of multidrug resistance, *Pseudomonas aeruginosa* infections require alternative therapeutics. The injectisome (iT3SS) and flagellar (fT3SS) type III secretion systems are 2 virulence factors associated with poor clinical outcomes. iT3SS translocates toxins, rod, needle, or regulator proteins, and flagellin into the host cell cytoplasm and causes cytotoxicity and NLRC4-dependent inflammasome activation, which induces interleukin 1β (IL–1β) release and reduces interleukin 17 (IL-17) production and bacterial clearance. fT3SS ensures bacterial motility, attachment to the host cells, and triggers inflammation. INP1855 is an iT3SS inhibitor identified by in vitro screening, using *Yersinia pseudotuberculosis*. Using a mouse model of *P. aeruginosa* pulmonary infection, we show that INP1855 improves survival after infection with an iT3SS-positive strain, reduces bacterial pathogenicity and dissemination and IL–1β secretion, and increases IL-17 secretion. INP1855 also modified the cytokine balance in mice infected with an iT3SS-negative, fT3SS-positive strain. In vitro, INP1855 impaired iT3SS and fT3SS functionality, as evidenced by a reduction in secretory activity and flagellar motility and an increase in adenosine triphosphate levels. As a result, INP1855 decreased cytotoxicity mediated by toxins and by inflammasome activation induced by both laboratory strains and clinical isolates. We conclude that INP1855 acts by dual inhibition of iT3SS and fT3SS and represents a promising therapeutic approach.

Keywords. *Pseudomonas aeruginosa*; type III secretion system; flagellum; pulmonary infection; cytotoxicity; inflammasome activation; anti-virulence strategy.

Multidrug resistance in *Pseudomonas aeruginosa* is spreading worldwide, encouraging research on alternative therapeutic strategies [1]. In this context, targeting virulence is appealing because disarming bacteria rather than killing them may reduce their pathogenicity while avoiding emergence of resistance. Type III secretion systems (T3SSs) represent a specialized class of secretion machines dedicated to assembly of injectisomes and flagella [2]. *P. aeruginosa* has 2 T3SSs, namely iT3SS (translocating effectors in the host cells) and fT3SS (ensuring bacterial motility).

The iT3SS is associated with poor clinical outcome in acute infections [3]. iT3SS is made of a syringe-like machine injecting bacterial toxins (ExoU or ExoS, ExoT, and ExoY) from the bacterial cytosol directly into the host cell by the concerted action of a needle complex and a translocon (proteins PopB, PopD, and PcrV). ExoU is a phospholipase A2 causing rapid cell death by altering membrane integrity, while ExoS and ExoT cause disruption of actin filaments (thereby preventing phagocytosis) and cytotoxicity (ExoS mainly). ExoY also contributes to actin cytoskeleton disorganization [4]. Importantly, iT3SS translocates other bacterial proteins, such as FliC (the monomeric subunit of flagellum), into the host cell cytosol [5, 6], which activate the cytosolic sensor NLRC4 (NLR family, CARD domain containing 4) inflammasome, resulting in pyroptosis [7]. Although the hypothesis is controversial [7], NLRC4 inflammasome activation and the subsequent release of interleukin 1β (IL-1β) and interleukin 18 is thought to contribute to lung injury and impaired *P. aeruginosa* clearance by reducing interleukin 17 and antimicrobial peptides production [8–10]. Last, iT3SS regulates its own expression (Supplementary Figure 1) [11]. Under inducing conditions, iT3SS secretes the negative regulator ExsE, liberating the anti-antiactivator ExsC and allowing it to displace the negative regulator ExsD from its binding to the transcriptional activator ExsA, allowing thereby iT3SS gene transcription.

fT3SS consists of a membrane-anchored basal body forming the flagellum, required for bacterial motility, adhesion to host

cells, bacterial dissemination, or initiation of inflammatory response [1, 12]. iT3SS and fT3SS share several general features. Their assembly depends on a T3SS located in the inner membrane and occurs following a similar process. Proteins directly involved in the secretion activity of iT3SS and the export activity of fT3SS share a high degree of similarity [13].

Inhibiting T3SS is thus an attractive therapeutic strategy [14]. However, no low-molecular-weight inhibitor has been evaluated so far against *P. aeruginosa* in vivo. Hydroxyquinolines inhibit iT3SS gene expression in *Yersinia pseudotuberculosis* and *Chlamydia trachomatis* [15] but have not been studied against *P. aeruginosa*. Among them, INP1855 (Figure 1A) was the most effective inhibitor of iT3SS gene expression in *Y. pseudotuberculosis*. The present study aims to evaluate INP1855 efficacy in a murine model of pseudomonal acute pulmonary infection and to assess how it modulates pathogen–host cell interactions.

MATERIALS AND METHODS

T3SS Inhibitor

INP1855 was provided by Creative Antibiotics Sweden (Umeå, Sweden). Stock solutions were prepared in dimethyl sulfoxide (DMSO; 10–16 mM) and stored at room temperature in the dark for <1 month.

In Vitro Studies

Bacteria, Cells, and Culture Conditions

Strains and plasmids are shown in Table 1. Twenty clinical isolates were collected from acute infections [16]. All strains were grown in lysogeny broth (LB) at 37°C with constant shaking (130 rpm). Growth curves were determined starting from overnight cultures resuspended in LB supplemented with INP1855 or its vehicle and adjusted to an OD_{620nm} of 0.1. The OD_{620nm} was followed over time while maintaining the culture at 37°C with aeration and constant shaking (300 rpm). Myelomonocytic THP-1 cells (ATCC TIB-202) [17] and alveolar epithelial A549 cells (ATCC CCL-185) [18] were grown in Roswell Park Memorial Institute 1640 medium and DMEM respectively, supplemented with 10% fetal calf serum. Adherent A549 cells were seeded in culture plates 2 days prior experiments.

Real-time Polymerase Chain Reaction (PCR)

Gene expression was measured as previously described [16], using the primers shown in Supplementary Table 1 and starting from cultures at an OD_{620nm} of 0.8 in LB plus 5 mM EGTA and 20 mM $MgCl_2$.

Western Blots

Bacteria were cultivated as for real-time PCR experiments. Proteins were collected [16] after separation of bacteria by centrifugation (for 15 minutes at 20 800 g). Supernatants were concentrated by centrifugation (for 10 minutes at 4000 g) through Amicon Ultra 4 centrifugal filters. Proteins were measured using the Bradford assay, and Western blots were performed as described elsewhere [16], using the following antibodies: anti-ExoS (dilution, 1:5000; Agrisera, Vännäs, Sweden), anti-GSK (dilution, 1:1000; Cell Signaling Technology, Danvers, MA), anti-FliC (dilution, 1:100; InvivoGen, Toulouse, France), anti-DsbA1 [19] (dilution, 1:30), and appropriate horseradish peroxidase–coupled secondary antibodies. Blots were revealed by chemiluminescence. Band intensity was quantified using Image J software, version 1.47V (available at: http://imagej.nih.gov/ij/).

Motility Assay

These experiments were performed as previously described [20], starting from overnight cultures resuspended in LB with DMSO or INP1855 and grown from an OD_{620nm} of 0.1–0.8 with aeration and constant shaking (300 rpm).

ATP Assay

Bacteria were cultivated as for real-time PCR experiments. The ATP level was measured in lysates by bioluminescence, using the ATP Determination Kit (Molecular probes, Eugene, OR).

Cytotoxicity Assay

Cytotoxicity was determined by measuring the release of the cytoplasmic enzyme lactate dehydrogenase (LDH) in culture medium [16].

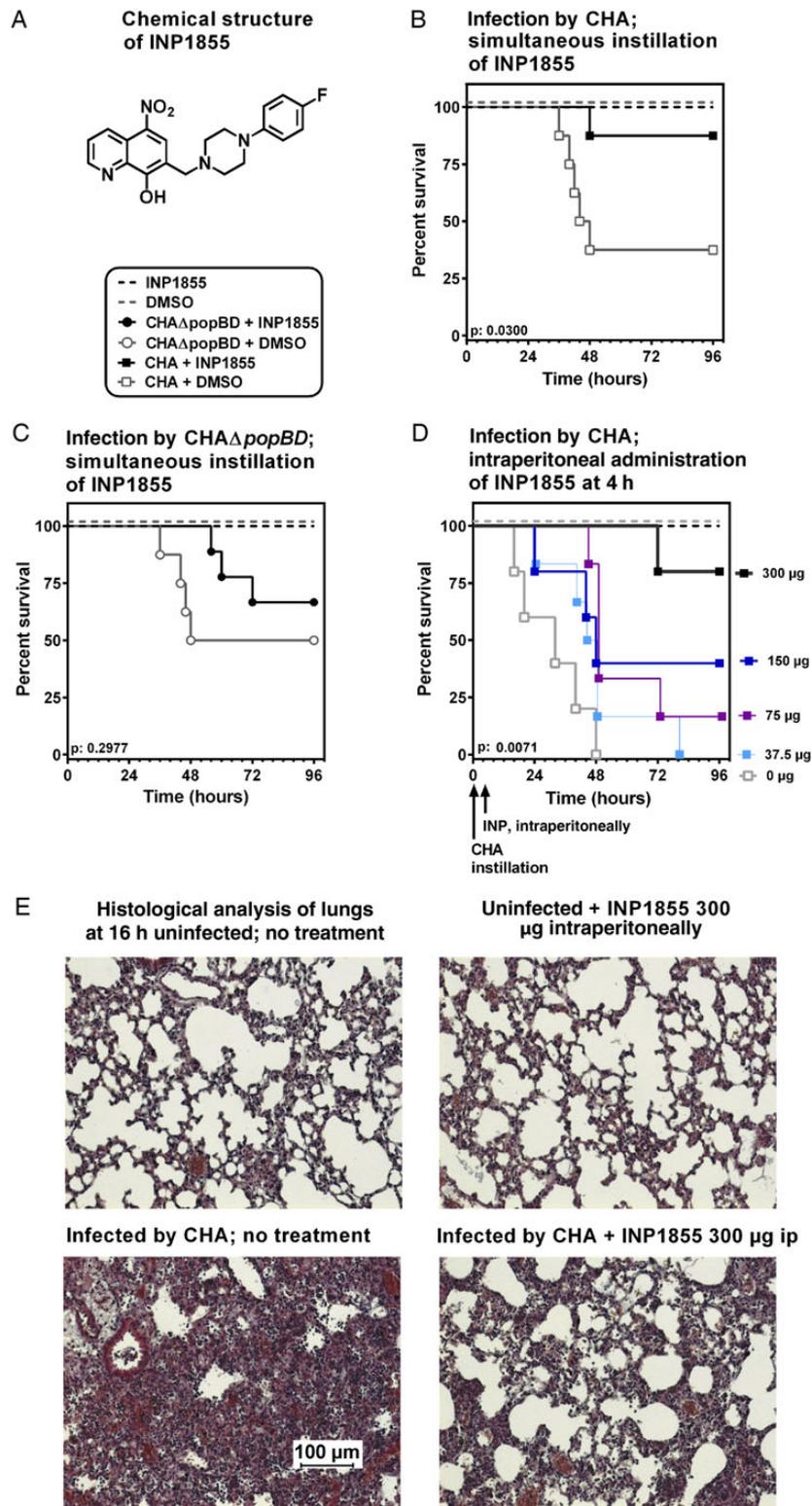### *P. aeruginosa* Internalization in THP-1 Cells

Overnight cultures were pretreated for 3 hours with INP1855 or DMSO, resuspended in Roswell Park Memorial Institute 1640 medium with 10% human serum in the presence of INP1855 or DMSO, and incubated for 1 hour at 37°C to allow opsonization [21]. Bacteria were added to monocytes in the presence of INP1855 or DMSO. Infected cells were incubated at 37°C for 2 hours to allow phagocytosis, washed in phosphate-buffered saline, and then exposed to 200 mg/L tobramycin for 1 hour to kill extracellular bacteria. Cells were washed in phosphate-buffered saline and lysed in sterile water, and aliquots were plated on agar for CFU determination after incubation at 37°C. Results were normalized per milligram of cell protein.

Inflammasome Activation and Flagellin Translocation in the Host Cells

Cytokine Assay

Except when stated otherwise, THP-1 cells were preincubated for 4 hours with 100 ng/mL lipopolysaccharide (LPS; to stimulate cytokine production) and 10 mg/L brefeldin A (to prevent interleukin 6 and tumor necrosis factor α (TNF-α) secretion [22]). Cytokine levels were measured by enzyme-linked immunosorbent assay (ELISA) [16] in supernatants of cells incubated for 5 hours with bacterial strains, INP1855, DMSO, nigericin, or combinations thereof.

Caspase-1 Activation and IL-1β Maturation

THP-1 monocytes were preincubated for 4 hours with 100 ng/mL LPS; incubated for 5 hours, as described for cytokine assays; and used for the study of caspase-1 activation or of IL-1β maturation. IL–1β was detected in cell lysates (pro-form) and extracellular medium (mature form). Western blots were performed as described

Figure 1. INP1855 reduces mortality in an acute model of lung infection in mice infected by CHA, an iT3SS- and fT3SS-positive *Pseudomonas aeruginosa* strain. *A*, Chemical structure of INP1855. *B–D*, Survival of wild-type mice intranasally infected with a lethal inoculum of CHA (1–2 × 10⁷ colony-forming units [CFU]; *B* and *D*) or of CHAΔ*popBD* (1 × 10⁸ CFU; *C*). As treatment, mice received either 1.67% dimethyl sulfoxide (DMSO; gray line) or INP1855 (4.5 µg; 10 nmol in 1.67% DMSO; black line) intranasally at the time of infection (*B* and *C*) or either 12.5% DMSO (gray line) or INP1855 at increasing doses (300, 150, 75, and 37.5 µg [660, 330, 165, and 82.5 nmol, respectively]) in 12.5% DMSO; black line) intraperitoneally 4 hours after the infection (*D*). The arrows below panel *D* show the timing of infection (CHA instillation) and treatment (INP, intraperitoneally). Plain lines denote infected mice, and dotted lines denote uninfected mice. Statistical analysis was performed by the log-rank test, comparing untreated and treated mice (n = 8 or 6 for each group of mice; 2 independent experiments were performed and showed similar results). *E*, Histological analysis of lungs from mice infected and treated as described in panel *D* (hematoxylin-eosin staining; original magnification ×100).

Table 1. Characteristics of *Pseudomonas aeruginosa* Reference Strains and Plasmids Used in This Study

| Strain or Plasmid | Description | T3SS Expression | | | FliC Expression | Reference |
| | | Translocation Apparatus | Toxins | | | |
			ExoS	ExoU		
Strain						
PA103	Wild-type, cytotoxic isolate; no flagellum	+	−	+	−	[40]
PA103ΔexsA	Ω element inactivation of exsA	−	−	−	−	[41]
PA103ΔexsD	Nonpolar deletion of exsD (in-frame deletion of codons 4–271 of exsD)	++[a]	−	++[a]	−	[42]
PA103ΔexsE	Nonpolar deletion of exsE (in-frame deletion of codons 4–78 of exsE)	++[a]	−	++[a]	−	[29]
PA103ΔUT	In-frame deletion of amino acids 330–571 of exoU and xylE aacC1 cassette replacing amino acids 36–348 of exoT; Gm[r]	+	−	−	−	[43]
PA103ΔpcrV	Tn5 Gm[r] cassette inserted into pcrV	−	−	+	−	[44]
CHA	Cystic fibrosis cytotoxic isolate	++	++	−	+	[45]
CHA (pC::lux)	lux fusion with exsCEBA promoter integrated at the attB site of the CHA chromosome	++	++	−	+	[46]
CHA (pS::lux)	lux fusion with exoS promoter at the attB site of the CHA chromosome	++	++	−	+	[46]
CHAΔfliC	fliC::gm mutant of CHA	++	++	−	−	This study
CHAΔexsA	exsA::gm mutant of CHA	−	−	−	+	[47]
CHAΔSTY	exoSTY::gm mutant of CHA	+	−	−	+	[8]
CHAΔpopBD	CHA with gentamicin resistance cassette inserted within popB and popD	−	+	−	+	[48]
CHAΔpopBDΔfliC	CHAΔpopBD strain with excision of lox sites and integration of new fliC::gm cassette	−	+	−	−	This study
Plasmid						
pUCPexsC	ExsC overexpression plasmid; Cb[r]	. . .	. . .	. . .	. . .	[49]
pUY44wt	Arabinose-inducible expression of ExsE-GSK; Gm[r]	. . .	. . .	. . .	. . .	[29]
pTRC99His-yscN	IPTG-inducible expression of His-YscN; Amp[r]	. . .	. . .	. . .	. . .	[50]

[a] Constitutive expression of iT3SS.

above, using the following primary antibodies: caspase-1 p10 (1:100; SantaCruz Biotechnology, Santa Cruz, CA), IL-1β (1:1000; R&D Systems), and anti-actin (Sigma–Aldrich) polyclonal antibody.

Flagellin Translocation

THP-1 cells were preincubated for 1 hour with cytochalasin D (to prevent phagocytosis) and incubated for 5 hours with bacteria in the presence of INP1855 or DMSO together with cytochalasin D. Cells were then centrifuged, washed, and incubated for 1 hour with tobramycin. FliC was detected by Western blot in cell lysates.

Animal Studies

C57BL/6J mice had free access to a chow diet in a temperature-controlled specified-pathogen-free environment, as determined by the Federation for Laboratory Animal Science Associations recommendations, with a half-day light cycle. Animals were lightly anesthetized with inhaled sevoflurane and infected by intranasal instillation of bacterial suspensions. INP1855 was administered either intranasally at the time of infection or intraperitoneally 4 hours later. Lung injury, bacterial burden and dissemination, cell counts, and cytokines in bronchoalveolar lavage (BAL) were determined using described procedures [8]. Histological analysis of lungs was performed using standard procedures and hematoxylin-eosin staining [23] in a blinded fashion.

Ethics Statement

Animal experiments were performed in an accredited establishment (N8 B59–108; Faculté de médecine de Lille, France) according to the governmental guidelines N886/609/CEE. They were approved by the local animal experimentation ethical committee of the région Nord-Pas-de-Calais (N8 CEEA 03/2004R). Animal care and procedures were in accordance with the French Guide for the Care and Use of Laboratory Animals and with the guidelines of the European Union.

Curve Fittings and Statistical Analyses

Curve fittings were performed with GraphPad Prism (version 6.05) and statistical analyses with GraphPad InStat (version 3.10) from GraphPad Software (San Diego, California).

RESULTS

Activity of INP1855 in Murine Acute Lung Infection

To demonstrate a protective effect of INP1855, mice were infected intranasally by CHA (iT3SS- and fT3SS-positive strain) and received at the same time a single dose of INP1855 (or its vehicle) by the same route. While survival was only 38% after 48 hours in CHA-infected mice receiving the vehicle, it reached 88% for INP1855-treated mice (Figure 1B). Survival was 50% in mice infected with a translocation-defective strain (CHAΔpopBD) and slightly (but not significantly) prolonged for those that received INP1855 (Figure 1C). To demonstrate

a therapeutic effect, INP1855 was administered intraperitoneally to CHA-infected animals 4 hours after the infection. A dose-dependent protective effect was observed (Figure 1D). INP1855 was innocuous for uninfected animals by both administration routes. Histological examination of lungs revealed a thickening of alveolar septa, an infiltration by inflammatory cells, and a loss of parenchyma organization in infected mice, which were reduced by INP1855 treatment (Figure 1E). To examine the INP1855 effect on bacterial dissemination and host response, mice were infected with sublethal inocula generating approximately 2%–3% injury in the lungs. In CHA-infected mice, INP1855 significantly reduced lung injury, bacterial burden, and dissemination to the spleen (Figure 2A); it did not change the total number of cells in BAL but decreased neutrophil and increased macrophage recruitment (Figure 2B). INP1855 also significantly decreased IL-1β and increased IL-17 levels in BAL without affecting TNF-α (Figure 2C; see Supplementary Figure 2 for additional inflammatory markers). In CHAΔ-popBD-infected mice, INP1855 significantly reduced dissemination to the spleen, neutrophils counts, and IL-1β and TNF-α levels in BAL and increased IL-17 levels. These parameters were less affected in mice infected with CHAΔpopBDΔfliC and were not modified by INP1855 (Supplementary Figure 3).

INP1855 Innocuity
Nonspecific toxic effects were ruled out by demonstrating that INP1855 did not modify CHA growth rate at concentrations of ≤250 μM and did not induce LDH release from THP-1 monocytes and A549 epithelial cells at concentrations of ≤60μM and after 5 (THP-1 cells) or 7 (A549 cells) hours of incubation (see Supplementary Figure 4, with justification of the incubation times).

Influence of INP1855 on Phagocytosis and Cytotoxicity
Because ExoS and ExoT inhibit bacterial internalization in eukaryotic cells [24, 25], we examined the effect of INP1855 on phagocytosis. INP1855 improved CHA internalization without affecting that of a strain that lacks iT3SS expression (CHA-ΔexsA; Supplementary Figure 5A). To evaluate the effect of INP1855 on CHA-induced cytotoxicity, we used THP-1 and A549 cells, which respond differently to infection by iT3SS-expressing strains [26] because A549 do not express NLRC4 [27], which is involved in inflammasome activation [28]. As shown in Supplementary Figure 5B, INP1855 decreased CHA cytotoxicity in a concentration-dependent manner in both cell types, reaching 40%–45% inhibition at 60 μM.

Using this fixed concentration, we evaluated the effect of INP1855 on the cytotoxicity of CHA, PA103, and selected mutants (Figure 3). Wild-type CHA and PA103 and mutants with constitutive iT3SS expression (PA103ΔexsD and PA103ΔexsE) were cytotoxic; this toxicity was significantly reduced by INP1855. Strains deleted for the translocation apparatus (CHAΔpopBD, PA103ΔpcrV) or the ExsA regulator (ΔexsA)

caused minimal LDH release, which was unchanged by INP1855. Strains deleted for toxins (CHAΔSTY and PA103ΔUT) were selectively toxic for THP-1 cells (via inflammasome activation [16]), and this toxicity was reduced by INP1855 as for parental strains.
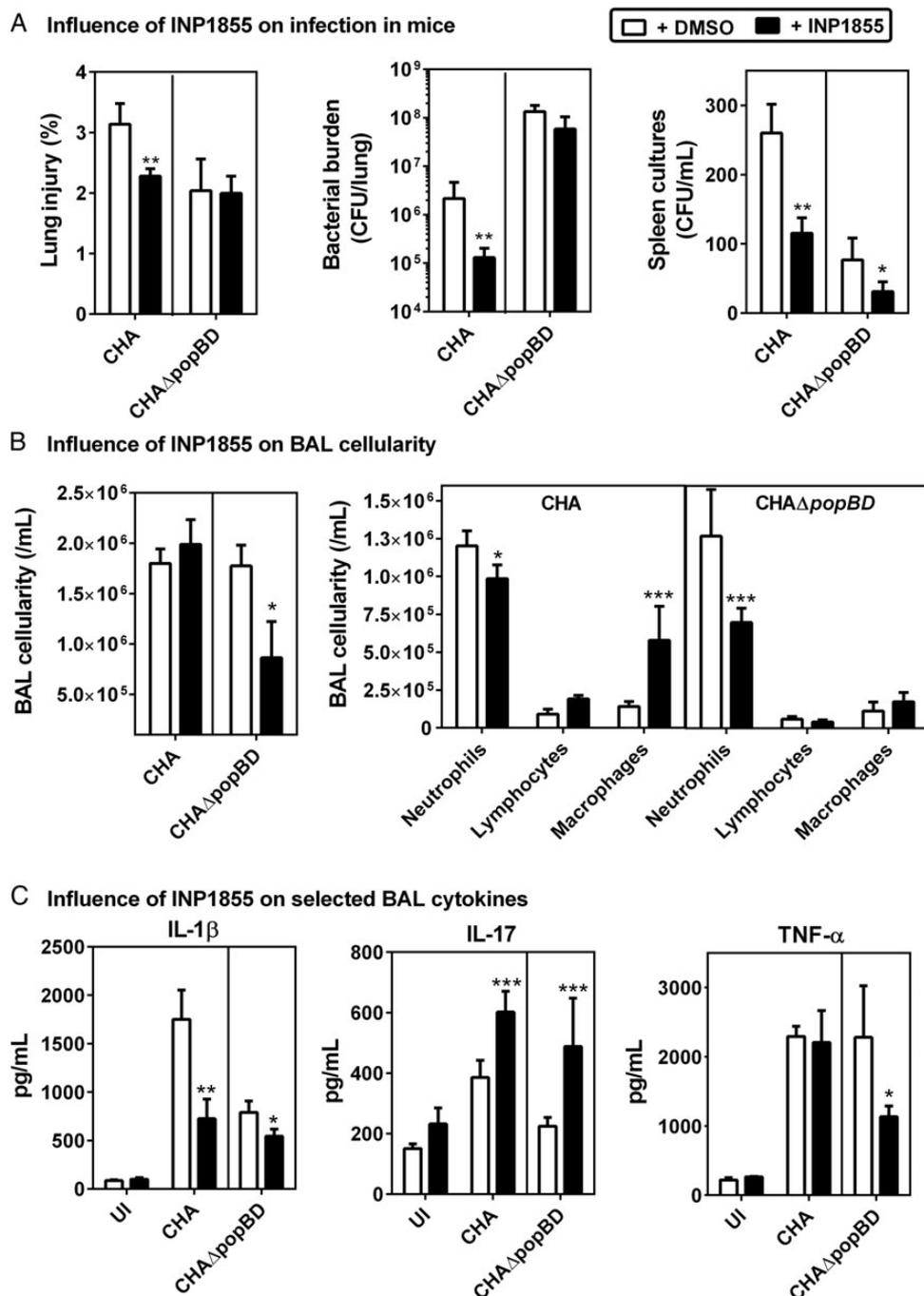
Influence of INP1855 on Gene Transcription
The mRNA levels for genes encoding iT3SS toxins (exoS, exoU [PA103], and exoT [both strains]) or the translocation apparatus (popB, popD, and pcrV) were measured in CHA, PA103, and its constitutive mutants (PA103ΔexsD and PA103ΔexsE; Figure 4A). INP1855 reduced the expression of these genes in CHA or PA103 by 20%–50% (these results were confirmed using a bioluminescent reporter strain, which also allowed us to show that this inhibition was concentration dependent [Supplementary Figure 6]). Of note, INP1855 was not a general inhibitor of transcription since it did not affect the expression of other genes, such as lasR and rhlR (quorum sensing regulators; determined in CHA [Figure 4A]). INP1855 did not change iT3SS gene expression in PA103ΔexsD (data not shown) and PA103ΔexsE, indicating that it does not directly act on iT3SS transcription but rather perturbs the ExsACDE regulatory cascade. Last, the effect of INP1855 on iT3SS gene transcription was not influenced by Phe-Arg-β-naphthylamide, a nonspecific efflux pump inhibitor, suggesting that INP1855 is not a substrate for efflux pumps (data not shown).

Influence of INP1855 on iT3SS Secretory Activity, Flagellar Motility, and Bacterial ATP Content
The effect of INP1855 was examined on the secretion of 3 proteins, namely ExoS, FliC, and ExsE, comparing their relative abundance in lysates from bacterial pellets and culture supernatants. With no anti-ExsE antibody available, we used a CHA strain transformed with the pUY44wt plasmid encoding ExsE coupled to a GSK tag [29]. INP1855 caused a concentration-dependent reduction in ExoS, FliC, and ExsE abundance in supernatants and a commensurate increase of their abundance in pellets (Figure 4B). Supernatants were not contaminated by nonsecreted proteins, since the inner membrane protein DsbA1 was detected in pellets only (Supplementary Figure 7).
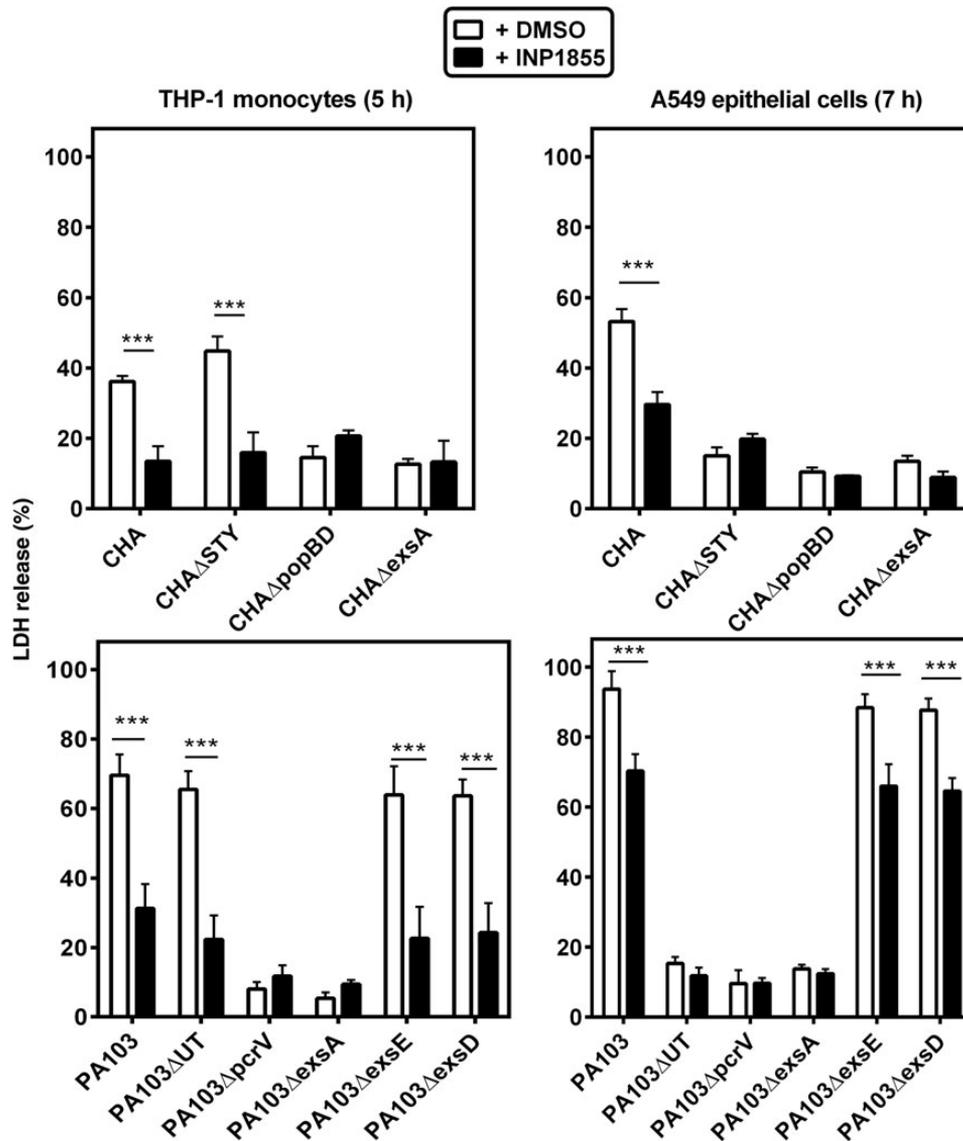
Assembly of the bacterial flagellum depends upon another T3SS (fT3SS) [13]. We therefore studied the effect of INP1855 on flagellar motility. INP1855 reduced swimming of CHA in a concentration-dependent manner (Figure 4C); it also impaired swarming of CHA and CHAΔexsA (Supplementary Figure 8). Of note, a strong correlation was observed between the capacity of INP1855 to inhibit iT3SS secretory activity and fT3SS-mediated motility (Supplementary Figure 9). Collectively, these data suggest that INP1855 inhibits both iT3SS and fT3SS. Since both systems require an ATPase, we measured ATP levels in flagellated CHA and unflagellated PA103 and their exsA deletion mutants (Figure 4D). INP1855 significantly increased ATP content in CHA, PA103, and CHAΔexsA but not in PA103ΔexsA, which has neither iT3SS nor fT3SS. Because the ATPases of

Figure 2. INP1855 decreases bacterial burden and dissemination and modulates host responses in an acute model of lung infection in mice, as revealed by a comparison of infection with the iT3SS-positive CHA strain and its Δ*popBD* mutant. Mice were intranasally infected with a nonlethal inoculum of CHA (5×10^6 colony-forming units [CFU]) or of CHAΔpop*BD* (5×10^7 CFU) and received a concomitant treatment with either 4.5 µg (10 nmol) INP1855 (black bars) dissolved in 1.67% dimethyl sulfoxide (DMSO) or 1.67% DMSO only (white bars) by the same route; mice were euthanized after 16 hours. Two independent experiments were performed and showed similar results. *A*, Lung injury index assessed by alveolar capillary barrier permeability, bacterial burden in the lungs after 24-hour culture, and bacterial dissemination assessed by spleen culture homogenates. Data are means ± SD (n = 5). *B*, Cell counts in bronchoalveolar lavage (BAL) fluid. Data are means ± SD (n = 5). *C*, Abundance of interleukin 1β (IL-1β), interleukin 17 (IL-17), and tumor necrosis factor α (TNF-α), measured by enzyme-linked immunosorbent assay in supernatants of BAL fluid. Data are means ± SD (n = 10). *P< .05, **P< .01, and ***P< .001, by the *t* test (when comparing untreated and treated mice) or 2-way analysis of variance with the Bonferroni post hoc test (when comparing cell types in BAL fluid). Abbreviation: UI, uninfected animals.

both T3SSs are highly homologous [13], we wondered whether INP1855 could inhibit these enzymes. Because the purified T3SS ATPase from *P. aeruginosa* was not available, we used YscN, the homologous iT3SS ATPase from *Y. pseudotuberculosis.* INP1855 caused a time- and concentration-dependent inhibition of this enzyme (Supplementary Figure 10).
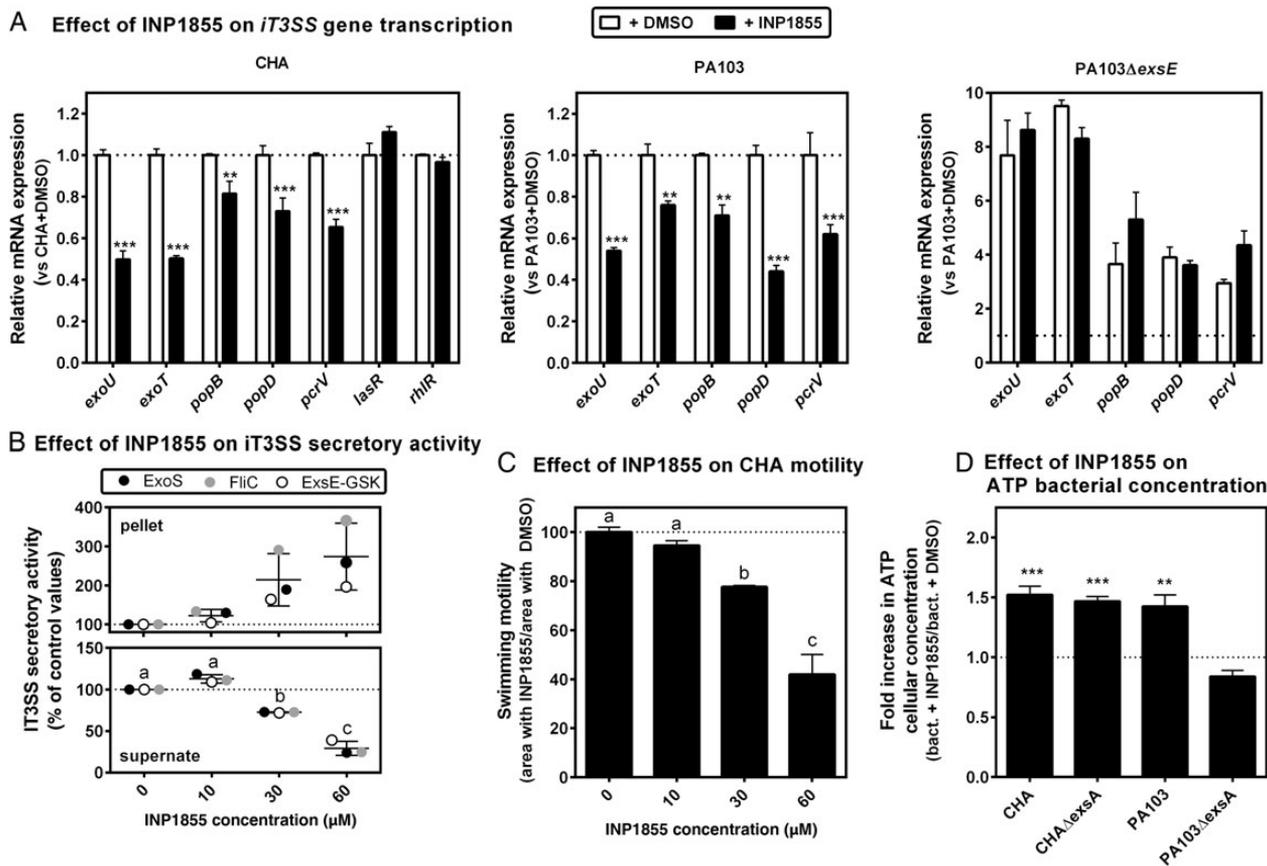
Figure 3. INP1855 inhibits iT3SS-mediated cytotoxicity. Effect of 60 µM INP1855 on cytotoxicity induced by different *Pseudomonas aeruginosa* strains in THP–1 monocytes (left) or A549 cells (right) after incubation for 5 and 7 hours, respectively. Values are expressed as the percentage of lactate dehydrogenase (LDH) released (when compared to the value measured for cells exposed to a lysis buffer [100% value]) and are mean ± standard error of the mean of 3 experiments performed in quadruplicate. ***$P < .001$, by 2-way analysis of variance with the Bonferroni post hoc test, for comparison between control conditions (dimethyl sulfoxide [DMSO]; open bars) and cells incubated with INP1855 (closed bars).

Influence of INP1855 on Inflammasome Activation in THP-1 Cells

The protective effect of INP1855 on cytotoxicity of CHAΔSTY and PA103ΔUT (expressing no toxins) for THP-1 cells (Figure 3) could result from an inhibition of inflammasome activation (Supplementary Figure 11) [8]. Flagellin translocation was therefore studied by Western blot in THP-1 cells incubated with CHA, CHAΔpopBD, or CHAΔfliC in the presence of INP1855 (Figure 5A). A strong signal was observed only for cells exposed to CHA, and its intensity was reduced by 45% by INP1855. We then examined the effect of INP1855 on caspase-1 activation and on release and maturation of IL–1β in the supernatant of THP-1 monocytes incubated with CHA and CHAΔSTY. Both

strains induced caspase-1 activation (Figure 5B) and maturation and release of IL–1β (Figure 5C), and these effects were impaired by INP1855. IL–1β was also measured by ELISA in supernatants of cell cultures exposed to CHA, CHAΔSTY, CHAΔpopBD, and CHAΔexsA. TNF-α was studied as a control because its secretion depends on the nuclear factor–κB pathway [30], rather than on inflammasome activation (Figure 5D). Nigericin was used in parallel as an inducer of NLRP3 inflammasome [31] to test for INP1855 specificity. Among the bacterial strains, only CHA and CHAΔSTY induced IL–1β release, which was inhibited by INP1855. Nigericin also caused caspase-1 activation (Supplementary Figure 12) and IL-1β release

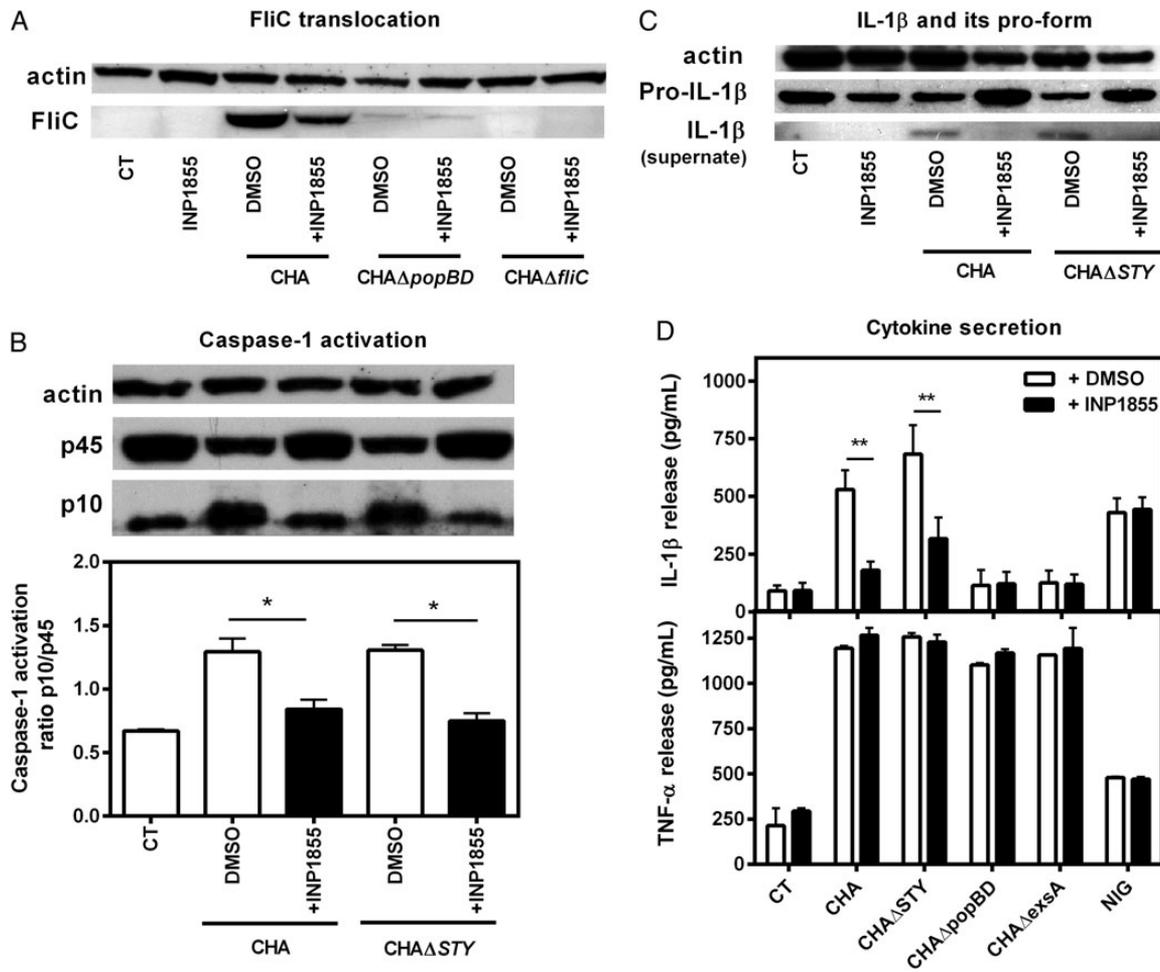**Figure 4.** INP1855 decreases nonconstitutive *iT3SS* transcription, secretion of ExoS and ExsE, and motility in iT3SS-expressing strains, and increases adenosine triphosphate (ATP) content in iT3SS- or fT3SS-expressing strains. *A*, Influence of INP1855 on iT3SS gene transcription. Messenger RNA (mRNA) levels of T3SS toxin (*exoS*, *exoU*, and *exoT*), T3SS translocation apparatus (*popB*, *popD*, and *pcrV*), or QS transcriptional activator (*lasR* and *rhlR*) genes as determined by real-time polymerase chain reaction. CHA, PA103, and PA103Δ*exsE* were grown from cultures at OD$_{620nm}$ values of 0.1–0.8 with constant shaking in the presence of 0.6% dimethyl sulfoxide (DMSO; vehicle) or 60 μM of INP1855 in 0.6% DMSO in low calcium medium (lysogeny broth, EGTA 5 mM, and MgCl$_2$ 20 mM) at 37°C to stimulate *iT3SS* expression and secretory activity. Results are expressed as relative messenger RNA (mRNA) expression levels when compared to controls (CHA and PA103 grown in the absence of INP1855). Dotted lines indicate the basal expression levels in CHA or PA103. Values represent the mean ± standard error of the mean of 2 experiments performed in duplicate. ***P < .001, **P < .01, and *P < .05, by 2-way analysis of variance (ANOVA) with the Bonferroni post hoc test, for comparison of values measured in control conditions or in the presence of INP1855. *B*, Effect of INP1855 on ExoS, FliC, and ExsE secretion. CHA and CHA expressing ExsE-GSK were grown from cultures at OD$_{620nm}$ values of 0.1–0.8 with constant shaking in the presence of 0.6% DMSO (control) or increasing concentrations of INP1855 in 0.6% DMSO in low-calcium medium containing arabinose 0.4%, gentamicin 100 mg/L, and carbenicillin 300 mg/L for CHA transformed with the pUY44wt and pUCPexsC plasmids. ExoS and FliC were detected by Western blot after separation by sodium dodecyl sulfate polyacrylamide gel electrophoresis (SDS-PAGE) of 2.5 μg (supernatants) or 5 μg of (lysates) proteins, and ExsE-GSK was detected after separation by SDS-PAGE of 50 μg (supernatants and lysates) or of proteins, using an antibody recognizing both phosphorylated and unphosphorylated GSK tags (anti-GSK). Band intensity was quantified using Image J software (Supplementary Figure 7). *C*, Effect of INP1855 on swimming motility. CHA was grown from cultures at OD$_{620nm}$ values of 0.1–0.8 with constant shaking in the presence of 0.6% DMSO (vehicle) or of increasing concentrations of INP1855 in 0.6% DMSO, after which 3 μL of the cultures were placed in the center of 0.3% lysogeny broth plates and grown overnight at 37°C. The area covered by bacteria was evaluated using the Quantity one software (Biorad). Values are mean ± SD of triplicates or quadruplicates. *P* < .05, by 1-way ANOVA with the Tukey post hoc test, for data with different letters. *D*, Effect of INP1855 on ATP concentration. CHA (iT3SS and fT3SS), CHAΔ*exsA* (no iT3SS), PA103 (no fT3SS), and PA103Δ*exsA* (no iT3SS; no fT3SS) were grown from cultures at OD$_{620nm}$ values of 0.1–0.8 with constant shaking in the presence of 0.6% DMSO (vehicle) or of 60 μM of INP1855 in 0.6% DMSO. ATP concentrations were measured in bacterial lysates (basal ATP values [nM], CHA: 201 ± 42 nM; CHAΔ*exsA*: 169 ± 65 nM; PA103: 165 ± 16 nM; and PA103Δ*exsA*: 180 ± 104 nM). Data are expressed in multiples of the value measured for the strains in the absence of INP1855 and are mean ± standard error of the mean of 2 experiments performed in triplicate. ***P < .001 and **P < .01, by 2-way analysis of variance with the Bonferroni post hoc test, for comparison of values measured in control conditions or in the presence of INP1855.

(Figure 5*D*), but these effects were not reverted by INP1855. All strains, irrespective of whether they expressed the iT3SS, and the combination of LPS and nigericin increased TNF-α release, but this effect was not prevented by INP1855 (Figure 5*D*). Thus, INP1855 seemed to protect cells from iT3SS-induced NLRC4 inflammasome activation. Results obtained for THP-1 cells

incubated with PA103 and its mutants are presented in Supplementary Figure 13.

Influence of INP1855 on Cytotoxicity of Clinical Isolates
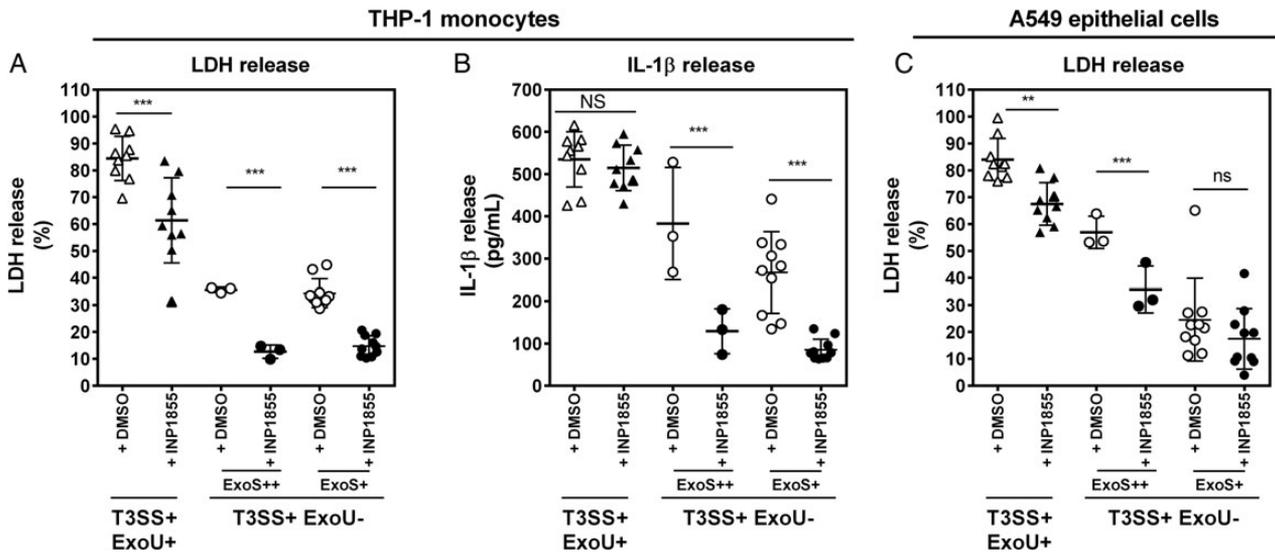We then examined the effects of INP1855 on LDH release (from THP-1 and A549 cells) and IL-1β release (from THP-1

Figure 5. INP1855 decreases flagellin translocation, caspase-1 activation, and interleukin 1β (IL-1β) maturation and secretion induced by iT3SS-positive strains without affecting tumor necrosis factor α (TNF-α) secretion. *A*, Effect of INP1855 on FliC translocation for CHA, CHAΔ*popBD*, and CHAΔ*fliC*. THP-1 cells were preincubated for 1 hour with cytochalasin D (1 mg/L) and then incubated for 5 hours with each strain (10 bacteria per cell) in the presence of 0.6% dimethyl sulfoxide (DMSO; vehicle) or 60 μM INP1855 and of 1 mg/L of cytochalasin D. Then, cells were centrifuged, washed, and incubated for 1 hour with tobramycin (200 mg/L). Cell lysates were separated by sodium dodecyl sulfate polyacrylamide gel electrophoresis and analyzed by Western blotting for the presence of FliC. Actin was detected in parallel for normalization purposes. The panel shows a representative gel out of 3 experiments. *B* and *C*, Effect of INP1855 on caspase-1 activation and IL-1β maturation or secretion induced by CHA and CHAΔ*STY*. THP-1 cells were preincubated for 4 hours in the presence of lipopolysaccharide (LPS; 100 ng/mL), after which cells were centrifuged, washed, and incubated for 5 hours with each strain (10 bacteria per cell) in the presence of 0.6% DMSO (vehicle) or 60 μM INP1855. Total cell lysates (45 μg protein) or supernatant (25 μg) were separated by SDS-PAGE and analyzed by Western blotting for the presence of the pro-form (45 kDa) and mature form (10 kDa) of caspase-1 (*B*) and for mature IL-1β (supernatant) and its pro-form (lysate; *C*). Actin was detected in parallel for normalization purposes. Band intensity was evaluated using Image J software. Each panel shows a representative gel out of 2 experiments. *D*, Influence of INP1855 on cytokine secretion. THP-1 monocytes were preincubated for 4 hours in the presence of LPS (100 ng/mL) and brefeldin A (10 mg/L), after which cells were centrifuged, washed, and incubated for 5 hours with the indicated bacterial strains (10 bacteria/cell) or nigericin (NIG; 0.02 μM) in the presence of 0.6% DMSO (vehicle) or 60 μM INP1855. IL-1β and TNF-α were then measured in the supernatant. All values are mean ± standard error of the mean (n = 3). **P < .01 and *P < .05, by 2-way analysis of variance with the Bonferroni post hoc test, for comparison of control conditions to INP1855.

cells) induced by clinical isolates collected from patients with acute infections (Figure 6) [16]. As previously observed [16], cytotoxicity was higher for strains expressing ExoU than those expressing ExoS. In THP-1 monocytes, INP1855 reduced cytotoxicity induced by ExoU-positive strains by 30% without impairing IL–1β release (the signal detected in this case corresponds to pro-IL-1β released from dead cells and is therefore not associated with inflammasome activation [16]). INP1855 also reduced cytotoxicity and IL-1β release by 65%–70% for strains expressing ExoS. In A549 epithelial cells, INP1855

reduced cytotoxicity by 18% and approximately 30% in strains expressing ExoU and ExoS, respectively.

DISCUSSION

This work is the first to study and assess the in vivo and in vitro activity of a pharmacological T3SS inhibitor against *P. aeruginosa*. In vivo, INP1855 shows protective effects against 4 hallmarks of iT3SS-mediated damage (mortality, lung injury, bacterial burden, and bacterial dissemination) [8, 9] in mice infected by an iT3SS-positive strain. It also reduces inflammation

Figure 6. INP1855 decreases the cytotoxicity of *Pseudomonas aeruginosa* clinical isolates. *A* and *C*, Percentage of lactate dehydrogenase (LDH) released from THP-1 monocytes (*A*) or A549 epithelial cells (*C*) exposed for 5 hours or 7 hours, respectively, to CHA, PA103, or 20 clinical isolates (10 bacteria/cell), in the presence of 0.6% dimethyl sulfoxide (DMSO; control; open symbol) or 60 µM INP1855 in 0.6% DMSO (closed symbols). *B*, Release of interleukin 1β (IL-1β) from THP-1 cells prestimulated with lipopolysaccharide (100 ng/mL) for 4 hours and then exposed for 5 hours to clinical isolates (10 bacteria/cell) in the presence of 0.6% DMSO (vehicle) or 60 µM INP1855 in 0.6% DMSO. Strains were grouped according to the expression of ExoU toxin (T3SS+ ExoU+ vs T3SS+ ExoU-) or ExoS toxin (ExoS++ : level of expression higher than that detected in CHA; ExoS+: level of expression lower than that detected in CHA [16]). Values are mean ± standard error of the mean of 3 independent experiments performed in quadruplicate (LDH) or duplicate (IL-1β). ***$P < .001$ and **$P < .01$, by 2-way analysis of variance with the Bonferroni post hoc test, for comparison of control conditions with INP1855. Abbreviation: NS, not significant.

in mice infected by an iT3SS-negative FliC-positive strain but not by a FliC-negative strain, suggesting that it may target both iT3SS and fT3SS. In vitro, INP1855 reduces iT3SS-dependent cytotoxicity mediated by toxins or by NLRC4 inflammasome activation. Thus, the use of INP1855 may represent a novel approach in antipseudomonal therapy.

Five pieces of evidence designate a core component of the iT3SS and fT3SS as a primary target of INP1855. First, INP1855 inhibits the secretion of iT3SS substrates (ExoS, FliC, and ExsE). Second, INP1855 impairs flagellar motility in both iT3SS-positive and iT3SS-negative strains, indicating an action unrelated to iT3SS inhibition. Third, INP1855 is equipotent to inhibit iT3SS secretory activity and fT3SS-mediated motility. Fourth, INP1855 increases ATP levels only in strains expressing iT3SS, fT3SS, or both systems. Fifth, INP1855 inhibits the ATPase activity of the homologous YscN enzyme from *Y. pseudotuberculosis* (57% and 47% identity with PscN and FliI, respectively [BLAST alignment]). Although inhibition of pseudomonal T3SS ATPases remains to be established, the fact that INP1855 inhibits the *Y. pseudotuberculosis* iT3SS [15] validates the use of YscN in our assays. Thus, these combined data suggest a possible specific mechanism of action for INP1855 and support the conclusion that INP1855 inhibits both the iT3SS and fT3SS by interacting with a common molecular target.

Translocation of ExsE is an initiating signal to induce iT3SS gene expression. Although INP1855 was originally identified as

an inhibitor of *iT3SS* transcription, our data show that its effect on this process is probably indirect (resulting from impaired ExsE secretion [32]), since INP1855 protects against PA103-Δ*exsE* cytotoxicity without affecting its gene expression. Another innovative observation is that INP1855 impairs caspase-1 activation and the subsequent IL-1β release induced by iT3SS-positive strains, 2 events related to NLRC4 inflammasome activation [5, 7–9]. Two experimental findings support inhibition of this cascade. First, INP1855 reverses the cytotoxicity of toxin-deleted mutants, which is strictly related to NLRC4 inflammasome activation [16]. Second, INP1855 inhibits caspase-1 activation and maturation of proIL–1β triggered by iT3SS-positive strains [16] but not by nigericin. This effect is consistent with a decreased delivery of the NLRC4 inflammasome activator flagellin. Moreover, the profile of cytokines in CHA-infected animals treated by INP1855 is similar to that described for NLRC4-deficient mice infected by CHA [8]. TNF–α is reduced in INP1855-treated mice infected by CHAΔ*popBD*, possibly reflecting an inhibition of TLR5 activation mediated by FliC. Likewise, the disbalance in immune cells observed in INP1855-treated animals (increase in macrophages/decrease in neutrophils) has been reported in IL-1β$^{-/-}$ mice infected by PA103ΔU [33] or in NLRC4$^{-/-}$ mice infected with CHA [8], suggesting that it could be a consequence of the impairment of IL-1β maturation and secretion.

In short, we propose that INP1855 acts as an antivirulence compound by specifically impairing the functionality of both

the iT3SS and the fT3SS (presumably by inhibiting the ATPase activity of their basal core) while only indirectly impairing iT3SS gene expression. This effect leads to reduced motility and increased phagocytosis of bacteria and to decreased cytotoxicity and inflammasome activation in the host cells (Supplementary Figure 14).

Compared with other antipseudomonal strategies [14], INP1855 may offer several advantages. First, it protects from cytotoxicity induced not only by toxins but also by the injectisome itself and may, therefore, display a broader spectrum of activity than antitoxin agents [34, 35]. Second, in contrast to antibodies specifically directed against injectisome proteins [36], INP1855 also inhibits flagellum-mediated toxicity, another determinant in pathogenicity [37, 38] (another drawback of antibodies is their unfavorable pharmacokinetics due to their proteic nature). Third, INP1855 is not a substrate for active efflux, which is a clear advantage over antibiotics [39]. Fourth, the changes in cytokine profile induced by INP1855 in mice are generally recognized as beneficial to the host. Although their findings are sometimes controversial [7, 23], animal and clinical studies demonstrate that high levels of IL–1β impair *Pseudomonas* clearance [9, 10]. Conversely, IL-17 stimulates the production of antimicrobial peptides [8].

Thus, pending for further investigations aimed at better characterizing the molecular targets of INP1855, examining its pharmacokinetic/pharmacodynamic profile, or evaluating its activity toward more-established infections, as well as in combination with antibiotics, this work could be considered as a first successful proof of concept that pharmacological inhibitors of T3SS may have beneficial effects on pseudomonal acute pulmonary infection by attenuating toxin effects and favorably modulating the host inflammatory response. In a biological context, studying the action of INP1855 also proved useful to better document the way *P. aeruginosa* interacts with its host.

Supplementary Data

Supplementary materials are available at http://jid.oxfordjournals.org. Consisting of data provided by the author to benefit the reader, the posted materials are not copyedited and are the sole responsibility of the author, so questions or comments should be addressed to the author.

Notes

References

1. Veesenmeyer JL, Hauser AR, Lisboa T, Rello J. Pseudomonas aeruginosa virulence and therapy: evolving translational strategies. Crit Care Med **2009**; 37:1777–86.
2. Diepold A, Armitage JP. Type III secretion systems: the bacterial flagellum and the injectisome. Philos Trans R Soc Lond B Biol Sci **2015**; 370:20150020.
3. El-Solh AA, Hattemer A, Hauser AR, Alhajhusain A, Vora H. Clinical outcomes of type III Pseudomonas aeruginosa bacteremia. Crit Care Med **2012**; 40: 1157–63.
4. Hauser AR. The type III secretion system of Pseudomonas aeruginosa: infection by injection. Nat Rev Microbiol **2009**; 7:654–65.
5. Miao EA, Ernst RK, Dors M, Mao DP, Aderem A. Pseudomonas aeruginosa activates caspase 1 through Ipaf. Proc Natl Acad Sci U S A **2008**; 105:2562–7.
6. Miao EA, Mao DP, Yudkovsky N, et al. Innate immune detection of the type III secretion apparatus through the NLRC4 inflammasome. Proc Natl Acad Sci U S A **2010**; 107:3076–80.
7. Sutterwala FS, Mijares LA, Li L, Ogura Y, Kazmierczak BI, Flavell RA. Immune recognition of Pseudomonas aeruginosa mediated by the IPAF/NLRC4 inflammasome. J Exp Med **2007**; 204:3235–45.
8. Faure E, Mear JB, Faure K, et al. Pseudomonas aeruginosa type-3 secretion system dampens host defense by exploiting the NLRC4-coupled inflammasome. Am J Respir Crit Care Med **2014**; 189:799–811.
9. Cohen TS, Prince AS. Activation of inflammasome signaling mediates pathology of acute P. aeruginosa pneumonia. J Clin Invest **2013**; 123:1630–7.
10. Schultz MJ, Rijneveld AW, Florquin S, Edwards CK, Dinarello CA, van der Poll T. Role of interleukin-1 in the pulmonary immune response during Pseudomonas aeruginosa pneumonia. Am J Physiol Lung Cell Mol Physiol **2002**; 282:L285–90.
11. Yahr TL, Wolfgang MC. Transcriptional regulation of the Pseudomonas aeruginosa type III secretion system. Mol Microbiol **2006**; 62:631–40.
12. Feldman M, Bryan R, Rajan S, et al. Role of flagella in pathogenesis of Pseudomonas aeruginosa pulmonary infection. Infect Immun **1998**; 66:43–51.
13. Blocker A, Komoriya K, Aizawa SI. Type III secretion systems and bacterial flagella: insights into their function from structural similarities. Proc Natl Acad Sci U S A **2003**; 100:3027–30.
14. Anantharajah A, Mingeot-Leclercq M-P, Van Bambeke F. Targeting type three secretion system in *Pseudomonas aeruginosa*. Trends Pharm Sci **2016**; doi:10.1016/j.tips.2016.05.11.
15. Enquist PA, Gylfe A, Hagglund U, et al. Derivatives of 8-hydroxyquinoline–antibacterial agents that target intra- and extracellular Gram-negative pathogens. Bioorg Med Chem Lett **2012**; 22:3550–3.
16. Anantharajah A, Buyck JM, Faure E, et al. Correlation between cytotoxicity induced by Pseudomonas aeruginosa clinical isolates from acute infections and IL-1beta secretion in a model of human THP-1 monocytes. Pathog Dis **2015**; 73:ftv049.
17. Tsuchiya S, Yamabe M, Yamaguchi Y, Kobayashi Y, Konno T, Tada K. Establishment and characterization of a human acute monocytic leukemia cell line (THP-1). Int J Cancer **1980**; 26:171–6.
18. Giard DJ, Aaronson SA, Todaro GJ, et al. In vitro cultivation of human tumors: establishment of cell lines derived from a series of solid tumors. J Natl Cancer Inst **1973**; 51:1417–23.
19. Arts IS, Ball G, Leverrier P, et al. Dissecting the machinery that introduces disulfide bonds in Pseudomonas aeruginosa. MBio **2013**; 4:e00912–913.
20. Wei Q, Tarighi S, Dotsch A, et al. Phenotypic and genome-wide analysis of an antibiotic-resistant small colony variant (SCV) of Pseudomonas aeruginosa. PLoS One **2011**; 6:e29276.
21. Buyck JM, Tulkens PM, Van Bambeke F. Pharmacodynamic evaluation of the intracellular activity of antibiotics towards Pseudomonas aeruginosa PAO1 in a

model of THP-1 human monocytes. Antimicrob Agents Chemother **2013**; 57:2310–8.

22. Schuerwegh AJ, Stevens WJ, Bridts CH, De Clerck LS. Evaluation of monensin and brefeldin A for flow cytometric determination of interleukin-1 beta, interleukin-6, and tumor necrosis factor-alpha in monocytes. Cytometry **2001**; 46:172–6.

23. Cai S, Batra S, Wakamatsu N, Pacher P, Jeyaseelan S. NLRC4 inflammasome-mediated production of IL-1beta modulates mucosal immunity in the lung against gram-negative bacterial infection. J Immunol **2012**; 188:5623–35.

24. Frithz-Lindsten E, Du Y, Rosqvist R, Forsberg A. Intracellular targeting of exoenzyme S of Pseudomonas aeruginosa via type III-dependent translocation induces phagocytosis resistance, cytotoxicity and disruption of actin microfilaments. Mol Microbiol **1997**; 25:1125–39.

25. Sundin C, Henriksson ML, Hallberg B, Forsberg A, Frithz-Lindsten E. Exoenzyme T of Pseudomonas aeruginosa elicits cytotoxicity without interfering with Ras signal transduction. Cell Microbiol **2001**; 3:237–46.

26. Coburn J, Frank DW. Macrophages and epithelial cells respond differently to the Pseudomonas aeruginosa type III secretion system. Infect Immun **1999**; 67:3151–4.

27. Vinzing M, Eitel J, Lippmann J, et al. NAIP and Ipaf control Legionella pneumophila replication in human cells. J Immunol **2008**; 180:6808–15.

28. Zhao Y, Shao F. The NAIP-NLRC4 inflammasome in innate immune detection of bacterial flagellin and type III secretion apparatus. Immunol Rev **2015**; 265: 85–102.

29. Urbanowski ML, Brutinel ED, Yahr TL. Translocation of ExsE into Chinese hamster ovary cells is required for transcriptional induction of the Pseudomonas aeruginosa type III secretion system. Infect Immun **2007**; 75:4432–9.

30. Leong KG, Karsan A. Signaling pathways mediated by tumor necrosis factor alpha. Histol Histopathol **2000**; 15:1303–25.

31. Petrilli V, Papin S, Dostert C, Mayor A, Martinon F, Tschopp J. Activation of the NALP3 inflammasome is triggered by low intracellular potassium concentration. Cell Death Differ **2007**; 14:1583–9.

32. Rietsch A, Vallet-Gely I, Dove SL, Mekalanos JJ. ExsE, a secreted regulator of type III secretion genes in Pseudomonas aeruginosa. Proc Natl Acad Sci U S A **2005**; 102:8006–11.

33. Al Moussawi K, Kazmierczak BI. Distinct contributions of interleukin-1alpha (IL-1alpha) and IL-1beta to innate immune recognition of Pseudomonas aeruginosa in the lung. Infect Immun **2014**; 82:4204–11.

34. Arnoldo A, Curak J, Kittanakom S, et al. Identification of small molecule inhibitors of Pseudomonas aeruginosa exoenzyme S using a yeast phenotypic screen. PLoS Genet **2008**; 4:e1000005.

35. Lee VT, Pukatzki S, Sato H, et al. Pseudolipasin A is a specific inhibitor for phospholipase A2 activity of Pseudomonas aeruginosa cytotoxin ExoU. Infect Immun **2007**; 75:1089–98.

36. Frank DW, Vallis A, Wiener-Kronish JP, et al. Generation and characterization of a protective monoclonal antibody to Pseudomonas aeruginosa PcrV. J Infect Dis **2002**; 186:64–73.

37. Patankar YR, Lovewell RR, Poynter ME, Jyot J, Kazmierczak BI, Berwin B. Flagellar motility is a key determinant of the magnitude of the inflammasome response to Pseudomonas aeruginosa. Infect Immun **2013**; 81:2043–52.

38. Rosok MJ, Stebbins MR, Connelly K, Lostrom ME, Siadak AW. Generation and characterization of murine antiflagellum monoclonal antibodies that are protective against lethal challenge with Pseudomonas aeruginosa. Infect Immun **1990**; 58:3819–28.

39. Nikaido H. Prevention of drug access to bacterial targets: permeability barriers and active efflux. Science **1994**; 264:382–8.

40. Liu PV. The roles of various fractions of Pseudomonas aeruginosa in its pathogenesis. 3. Identity of the lethal toxins produced in vitro and in vivo. J Infect Dis **1966**; 116:481–9.

41. Brutinel ED, Vakulskas CA, Yahr TL. ExsD inhibits expression of the Pseudomonas aeruginosa type III secretion system by disrupting ExsA self-association and DNA binding activity. J Bacteriol **2010**; 192:1479–86.

42. McCaw ML, Lykken GL, Singh PK, Yahr TL. ExsD is a negative regulator of the Pseudomonas aeruginosa type III secretion regulon. Mol Microbiol **2002**; 46:1123–33.

43. Garrity-Ryan L, Kazmierczak B, Kowal R, Comolli J, Hauser A, Engel JN. The arginine finger domain of ExoT contributes to actin cytoskeleton disruption and inhibition of internalization of Pseudomonas aeruginosa by epithelial cells and macrophages. Infect Immun **2000**; 68:7100–13.

44. Hauser AR, Fleiszig S, Kang PJ, Mostov K, Engel JN. Defects in type III secretion correlate with internalization of Pseudomonas aeruginosa by epithelial cells. Infect Immun **1998**; 66:1413–20.

45. Toussaint B, Delic-Attree I, Vignais PM. Pseudomonas aeruginosa contains an IHF-like protein that binds to the algD promoter. Biochem Biophys Res Commun **1993**; 196:416–21.

46. Shen DK, Filopon D, Kuhn L, Polack B, Toussaint B. PsrA is a positive transcriptional regulator of the type III secretion system in Pseudomonas aeruginosa. Infect Immun **2006**; 74:1121–9.

47. Dacheux D, Attree I, Schneider C, Toussaint B. Cell death of human polymorphonuclear neutrophils induced by a Pseudomonas aeruginosa cystic fibrosis isolate requires a functional type III secretion system. Infect Immun **1999**; 67:6164–7.

48. Goure J, Pastor A, Faudry E, Chabert J, Dessen A, Attree I. The V antigen of Pseudomonas aeruginosa is required for assembly of the functional PopB/PopD translocation pore in host cell membranes. Infect Immun **2004**; 72: 4741–50.

49. Dasgupta N, Lykken GL, Wolfgang MC, Yahr TL. A novel anti-anti-activator mechanism regulates expression of the Pseudomonas aeruginosa type III secretion system. Mol Microbiol **2004**; 53:297–308.

50. Davis AJ, Diaz DAD, Mecsas J. A dominant-negative needle mutant blocks type III secretion of early but not late substrates in Yersinia. Mol Microbiol **2010**; 76:236–59.

Inhibition of the injectisome and flagellar Type III Secretion Systems by INP1855 impairs *Pseudomonas aeruginosa* pathogenicity and inflammasome activation

Ahalieyah Anantharajah, Emmanuel Faure, Julien M. Buyck, Charlotta Sundin, Tuulikki Lindmark, Joan Mecsas, Timothy L. Yahr, Paul M. Tulkens, Marie-Paule Mingeot-Leclercq, Benoît Guery, Françoise Van Bambeke.
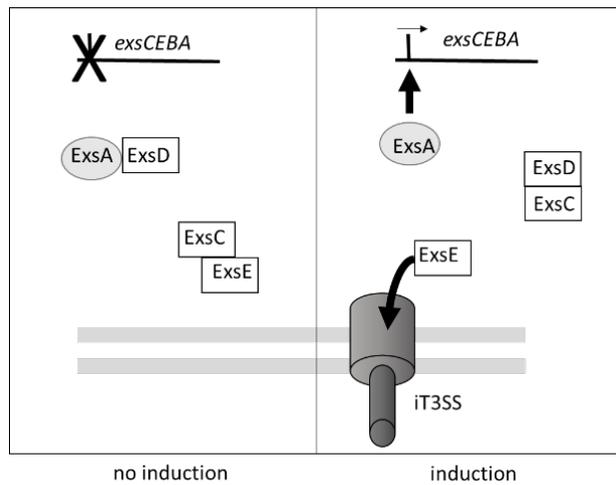
<mark>Supplementary material</mark>

Table S1: Primers used for Real time PCR

Primer	Sequence	
	F	**R**
rpsL*	CGGCACTGCGTAAGGTATGC	CGTACTTCGAACGACCCTGCT
exoS	GGCGGATGCGGAAAAGTAC	CTGACGCAGAGCGCGATT
exoT	ATGCGGTAATGGACAAGGTC	CTGGTACTCGCCGTTGGTAT
popB	CTTTGGTTGGATCAGTGCAA	CCGAGCTTTTCCATCACTTC
popD	ACACGGTGATCCAGTCCTTC	CTGGTTATGGCTCTGGGTGT
pcrV	CGATGAGTACCCCTTCGAGA	ATTTCTGGATGAAGCGGTTG
exoU	AGAACGGAGTCACCGAGCTA	CGAGCAGCGAAATAAGATCC
lasR	ACGCTCAAGTGGAAAATTGG	TCGTAGTCCTGGCTGTCCTT
rhlR	CTGGGCTTCGATTACTACGC	CCCGTAGTTCTGCATCTGGT

* used as housekeeping gene
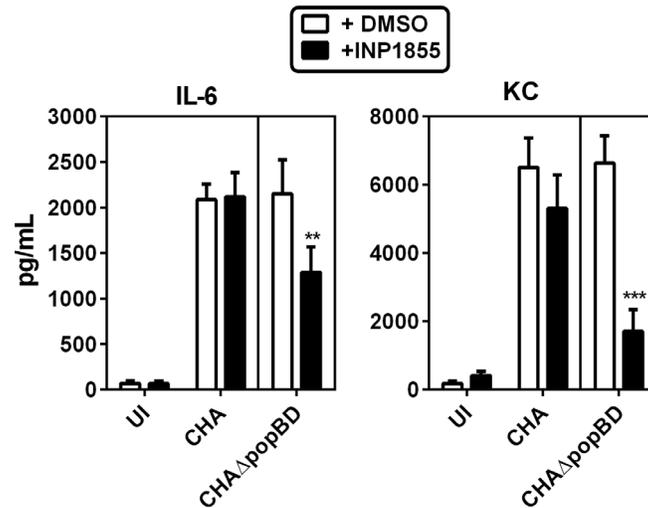
Figure S1 : regulation of iT3SS expression by ExsA

• ExsD is a negative regulator of ExsA
• ExsC is an anti-antiactivator binding to and inhibiting the negative regulatory activity of ExsD
• ExsE is a negative regulator of ExsC.

In the absence of environmental signals, ExsC preferentially binds to ExsE, and ExsD to ExsA, leading to an inhibition of ExsA-dependent transcription.

Under inducing conditions, ExsE is secreted by the iT3SS, releasing ExsC, which binds to ExsD, thereby liberating ExsA and activating iT3SS gene expression.

*Adapted from Yahr TL, Wolfgang MC. Transcriptional regulation of the Pseudomonas aeruginosa type III secretion system. Mol Microbiol. **2006**;62:631-40.*

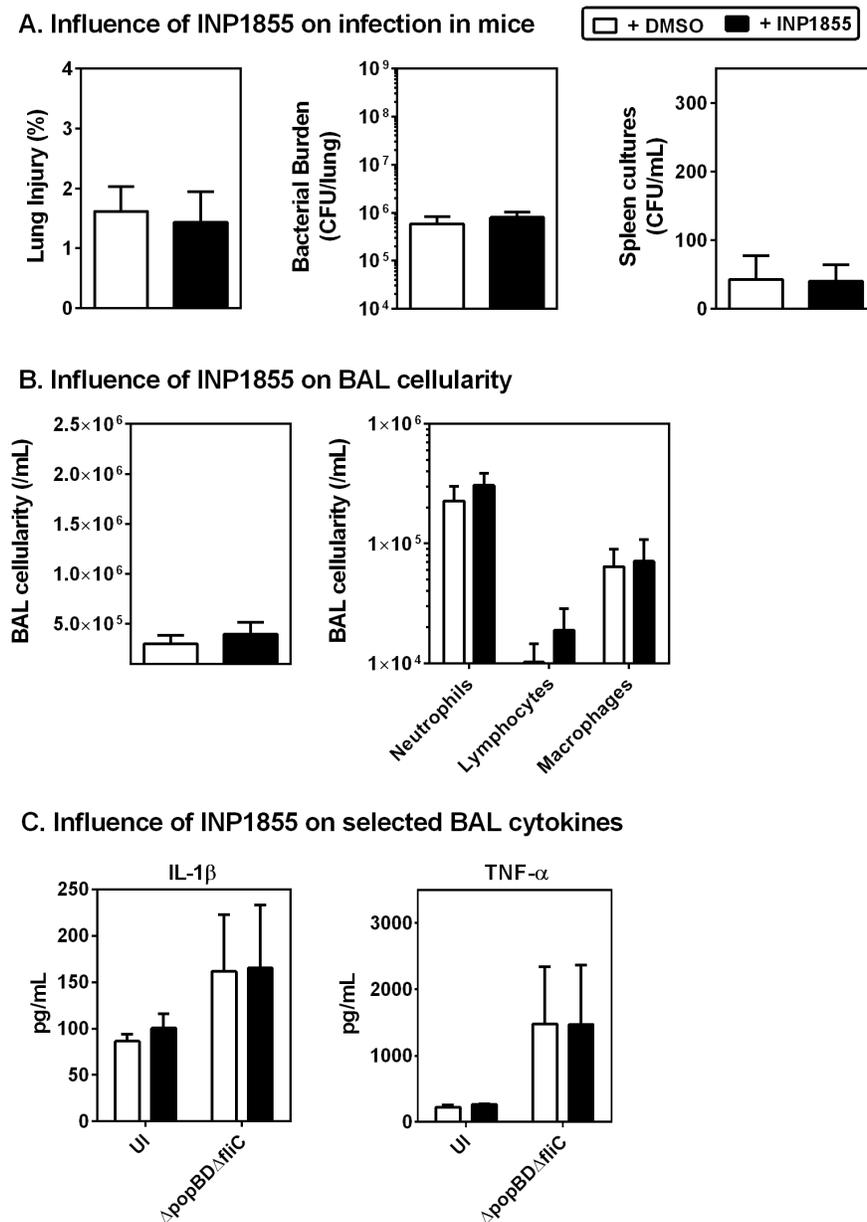**Figure S2**

Influence of INP1855 on IL-6 and KC (Keratinocyte Chemoattractant) levels in BAL of mice infected by CHA or CHAΔ*popBD*

Mice were intranasally infected with a non-lethal inoculum of CHA (5 x 10^6 CFU) or CHAΔ*popBD* (5 x10^7 CFU) and received a concomitant treatment with either 4.5 μg (10 nmol) INP1855 (black bars) dissolved in 1.67% DMSO or 1.67% DMSO only (white bars) by the same route; mice were sacrificed after 16h. Abundance of IL-6 and KC were measured by ELISA in supernatants of BAL fluids. UI: uninfected animals. Data are means ± SD (n = 10). Statistical analysis (two-way ANOVA, Bonferonni's post test; comparison between treated and untreated mice: ** $p<0.01$; *** $p<0.001$.

Figure S3

A. Influence of INP1855 on infection in mice

□ + DMSO ■ + INP1855

B. Influence of INP1855 on BAL cellularity

C. Influence of INP1855 on selected BAL cytokines

INP1855 does not affect pathogenicity and host response in an acute model of lung infection in mice infected by CHAΔ*popBD*Δ*fliC*.

Mice were intranasally infected with a non-lethal inoculum of CHAΔpop*BD*Δ*fliC* (5 x10^7 CFU) and received a concomitant treatment with either 4.5 µg (10 nmol) INP1855 (black bars) dissolved in 1.67% DMSO or 1.67% DMSO only (white bars) by the same route; mice were sacrificed after 16 h.

(A) Lung injury index assessed by alveolar capillary barrier permeability; bacterial burden in the lungs after 24-hour culture; bacterial dissemination assessed by spleen culture homogenates.
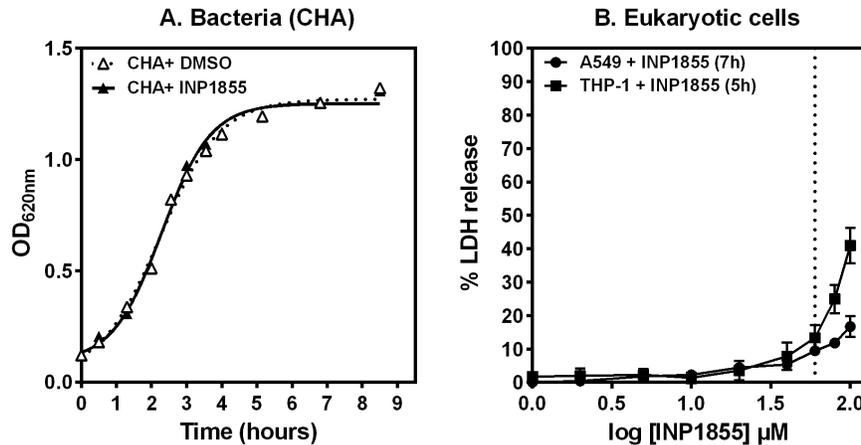(B) Cell counts in bronchoalveolar lavage (BAL) Data are means ± SD (n=5)
(C) Abundance of IL-1β and TNF-α measured by ELISA in supernatants of BAL fluids. UI: uninfected animals. Data are means ± SD (n = 10).
Statistical analysis (t-test when comparing untreated and treated mice or two ways ANOVA, Bonferonni's post test when comparing cell types in BAL): no difference observed.
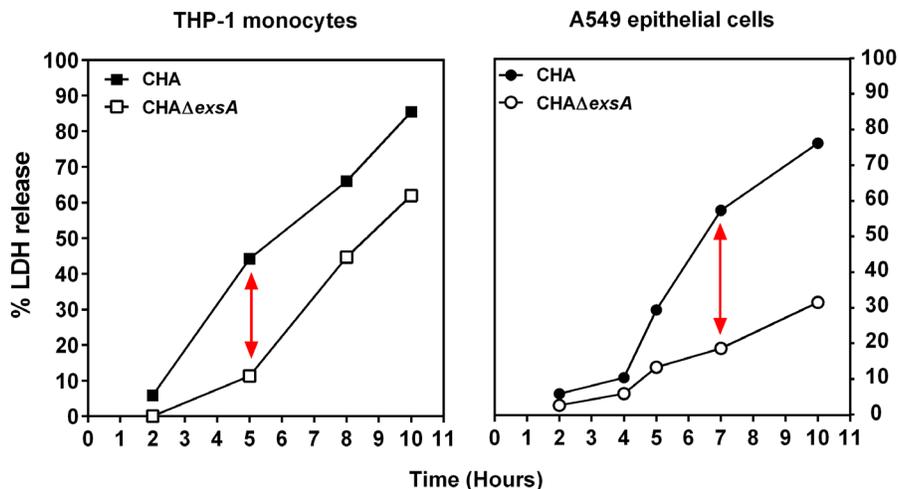
Figure S4

1. INP1855 does not affect bacterial growth neither eukaryotic cell viability at the concentrations used in this study.

A. Bacteria (CHA)

B. Eukaryotic cells

(A): Effect of INP1855 on viability of bacteria, as assessed by following over time the optical density at 620 nm of a suspension of CHA in the presence of 250 µM INP1855 or 2.5 % DMSO (vehicle).

(B): Effect of INP1855 on viability of eukaryotic cells, as assessed by measuring the release of LDH in the culture medium after 5 h (THP-1) or 7 h (A549) of incubation with increasing concentrations of INP1855.The vertical dotted line corresponds to the concentration of 60 µM used in most experiments.
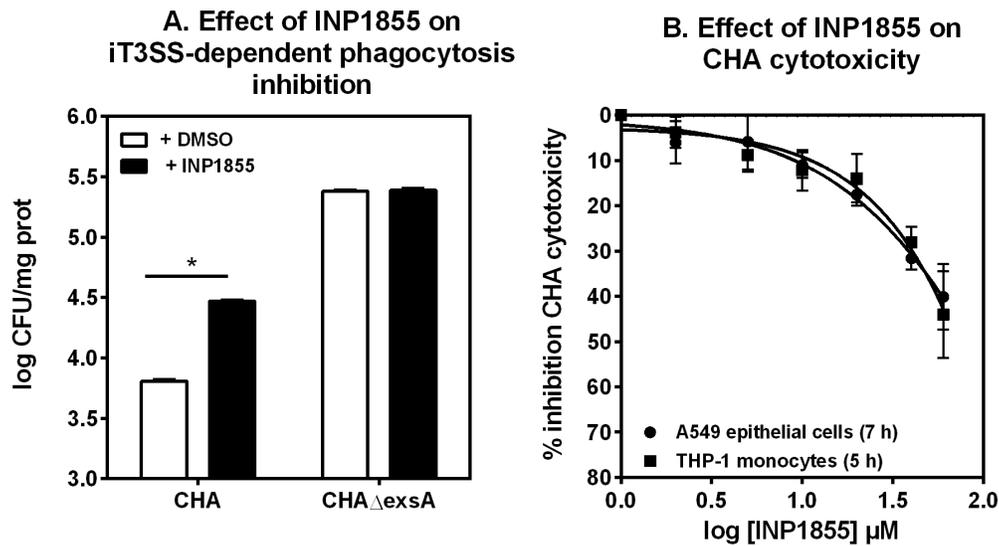
2. Kinetics of T3SS cytotoxicity towards phagocytic and epithelial cells.

THP-1 monocytes

A549 epithelial cells

Evolution of cell viability over time in cells incubated with CHA (expressing iT3SS) or CHAΔ*exsA* (not expressing T3SS) at an inoculum of 10 bacteria/cell. Cell viability was assessed by measuring the release of LDH in the culture medium of THP-1 monocytes (left panel) and A549 epithelial cells (right panel).

The red arrows indicate the times selected in further experiments, i.e. the time for which cytotoxicity was essentially mediated by T3SS (largest difference observed between CHA and CHAΔ*exsA* cytotoxicity and low cytotoxicity [< 20 %] for CHAΔ*exsA*).
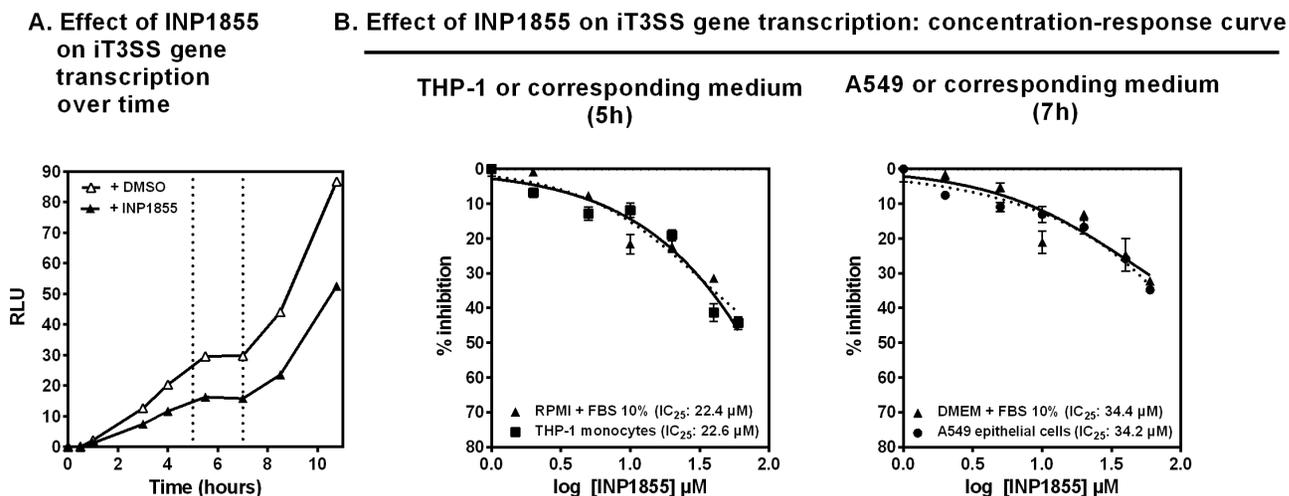
Figure S5

INP1855 antagonizes iT3SS-mediated (A) inhibition of bacterial internalization by THP-1 monocytes and (B) toxicity for eukaryotic cells.

(A) Effect of INP1855 on phagocytosis of CHA and CHA∆*exsA* by THP-1 cells. Bacteria were pretreated with 60 µM INP1855 in 0.6% DMSO or exposed to 0.6% DMSO (vehicle) for 3 h and then opsonised with human serum for 1h. Phagocytosis was allowed for 2h using an initial inoculum of 10 bacteria/cell in medium containing 60 µM INP1855 or 0.6% DMSO, after which non-phagocytosed bacteria were killed by incubation with 200 mg/L tobramycin for 1h. Values are the mean ± SEM of 2 experiments performed in triplicate. Statistical analysis (t-test):* p<0.05.

(B) Inhibition of CHA cytotoxicity by INP1855. Cell viability was assessed by measuring LDH release in the culture medium after 5h (THP-1) or 7h (A549) of incubation with CHA (10 bacteria/cell) and increasing concentrations of INP1855. Values represent the percent inhibition of CHA cytotoxicity (as measured in the absence of INP1855 and represent the mean ± SEM of 3 experiments performed in quadruplicates.

Figure S6

A. Effect of INP1855 on iT3SS gene transcription over time

B. Effect of INP1855 on iT3SS gene transcription: concentration-response curve

THP-1 or corresponding medium (5h)

A549 or corresponding medium (7h)

INP1855 decreases non-constitutive *iT3SS* transcription as determined using a bioluminescent reporter strain

Influence of INP1855 on expression of the *exsCEBA* operon, followed by measuring the bioluminescence signal of the reporter strain CHA*pC::lux*.
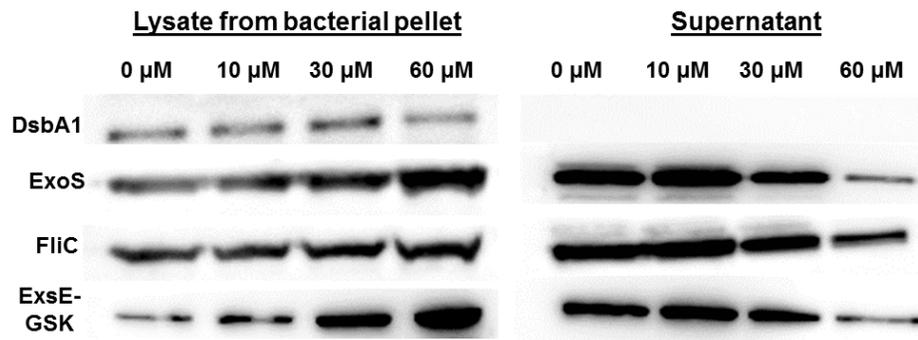
(A) Kinetics of bioluminescence over time in the presence of 0.6% DMSO (vehicle) or of 60 µM INP1855 in 0.6% DMSO and expressed in arbitrary units [RLU]) for bacteria cultured in low calcium medium (LB broth with 5 mM EGTA and 20 mM $MgCl_2$). A 40-50% reduction in the bioluminescent signal was observed in the presence of INP1855 throughout the experiment. The dotted lines indicate the times selected for the experiments in panel B.

(B) Inhibition of CHA*pC::lux* reporter activity by increasing concentrations of INP1855 measured after 5h of incubation in the presence of THP-1 monocytes (left; 10 bacteria/cell) or the corresponding culture medium (RPMI + 10% fetal calf serum), or 7h of incubation in the presence of A549 cells (right; 10 bacteria/cell) or the corresponding culture medium (DMEM + 10% fetal calf serum). Values are expressed as the percent inhibition of the luminescence signal recorded in the absence of INP1855 (19.2 and 17.8 RLU for THP-1 cells and the corresponding culture medium; 3.8 and 4.0 RLU for A589 cells or their corresponding culture medium, respectively). All values are the mean ± SEM of 2 or 3 experiments performed in duplicate or triplicate. The IC_{25} values were calculated from sigmoidal dose-response functions with variable slope as determined by non-linear regression using GraphPad Prism®.

Similar results were obtained with CHA*pS::lux* reporter strain (not shown)

Corresponding method: Overnight cultures of reporter bioluminescent strains were centrifuged and resuspended in (A) LB broth with 5 mM EGTA and 20 mM $MgCl_2$ or (B) in eukaryotic cell culture medium (supplemented by 10% of fetal calf serum) and added to THP-1 monocytes (5 x 10^5 cells/mL; 10 bacteria/cell) or A549 epithelial cells (2 x 10^4 cells/mL) in the presence INP1855 (up to 60 µM) in DMSO (maximal concentration: 0.6%) or in DMSO (at the same concentration as used with INP1855; vehicle). Plates were incubated without shaking at 37°C in a 5% CO_2 atmosphere. Luminescence (RLU) was measured over time a Victor X2 Multilabel Microplate reader (Perkin Elmer Life Science, Turku, Finland). Concentration-response curves were also obtained after 5 h (THP-1) or 7 h (A549) of incubation.
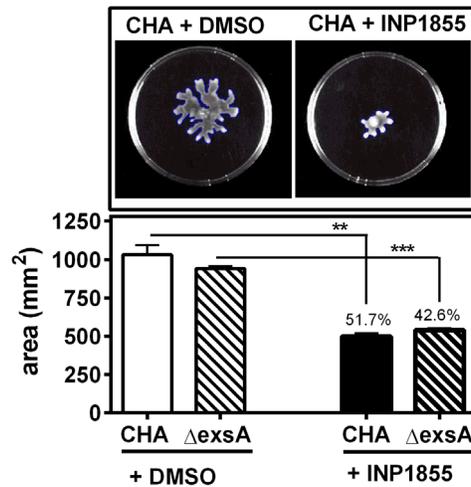
Figure S7

Effect of INP1855 at increasing concentrations on ExoS, FliC and ExsE secretion.

CHA or CHA expressing ExsE-GSK were grown from $OD_{620\ nm}$ 0.1 to 0.8 with constant shaking in the presence of 0.6% DMSO (control) or of 10 µM, 30 µM or 60 µM of INP1855 in low calcium medium (LB broth + EGTA 5 mM + $MgCl_2$ 20 mM) complemented with arabinose 0.4%, gentamicin 100 mg/L, and carbenicillin 300 mg/L for CHA expressing ExsE-GSK. Proteins were detected in lysates (left) or in supernates (right) using monoclonal antibodies directed against ExoS (1/5000), FliC (1/100), or GSK (1/1000). In order to check for the effectiveness of the centrifugation procedure to separate supernatants from bacteria, the non-secreted protein DsbA1 was detected in parallel (anti-DsbA1 diluted 1/30; Arts IS, Ball G, Leverrier P, Garvis S, Nicolaes V, Vertommen D, Ize B, Tamu Dufe V, Messens J, Voulhoux R, Collet JF. Dissecting the machinery that introduces disulfide bonds in *Pseudomonas aeruginosa.* MBio **2013**;4(6):e00912-13).
Control and highest INP1855 concentrations were tested independently 3-4 times with similar results.
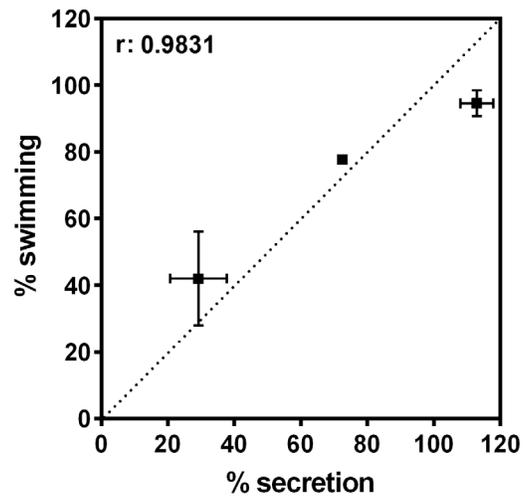
Figure S8

INP1855 decreases flagellar motility

Effect of INP1855 on swarming motility. CHA (illustrated in the pictures) and CHAe*xsA* were grown from $OD_{620\,nm}$ 0.1 to 0.8 with constant shaking in the presence of 60 µM of INP1855 in 0.6% DMSO or in 0.6 % DMSO (control), after which 3 µL of these cultures were placed in the center of 0.5 % agar LB plates and grown overnight at 37°C. The area covered by bacteria was evaluated using the Quantity one® software (Biorad). Values are mean ± SEM of 2 independent experiments performed in duplicate. Statistical analysis: ** $p<0.01$, *** $p<0.001$; Student t test comparing values measured in control conditions or in the presence of INP1855.

The same experiment was performed with CHAΔf*liC*, which did not show any swarming motility in the absence or in the presence of INP1855.
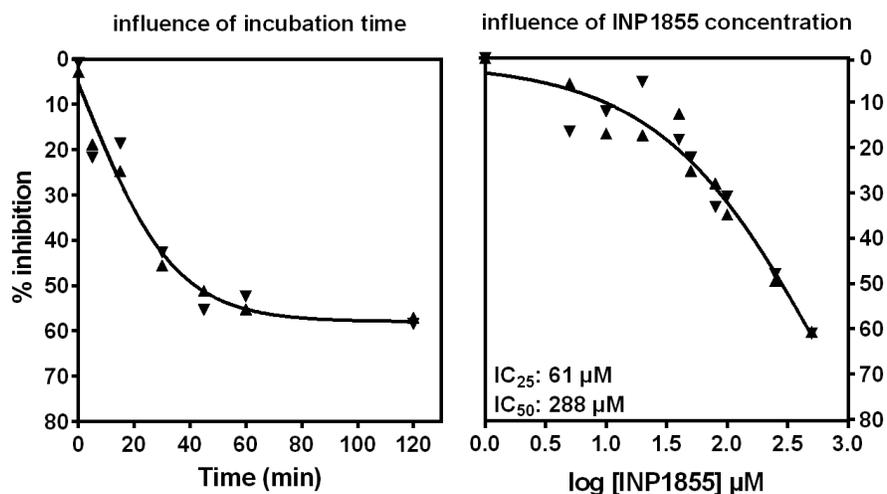
Figure S9

Comparison of the effect of INP1855 on secretion of proteins (ExoS, FliC, ExsE) by iT3SS and on swimming motility.

The graph uses the data presented in Figure 4 for bacteria exposed to increasing concentrations of INP1855 and expressed here as the percentage of secretion of iT3SS substrates (X axis) or of swimming mobility (Y axis) determined in the presence of INP1855 *vs.* control conditions (DMSO; no inhibitor added). The oblique dotted line represents equivalence of effects along the X and Y axes.

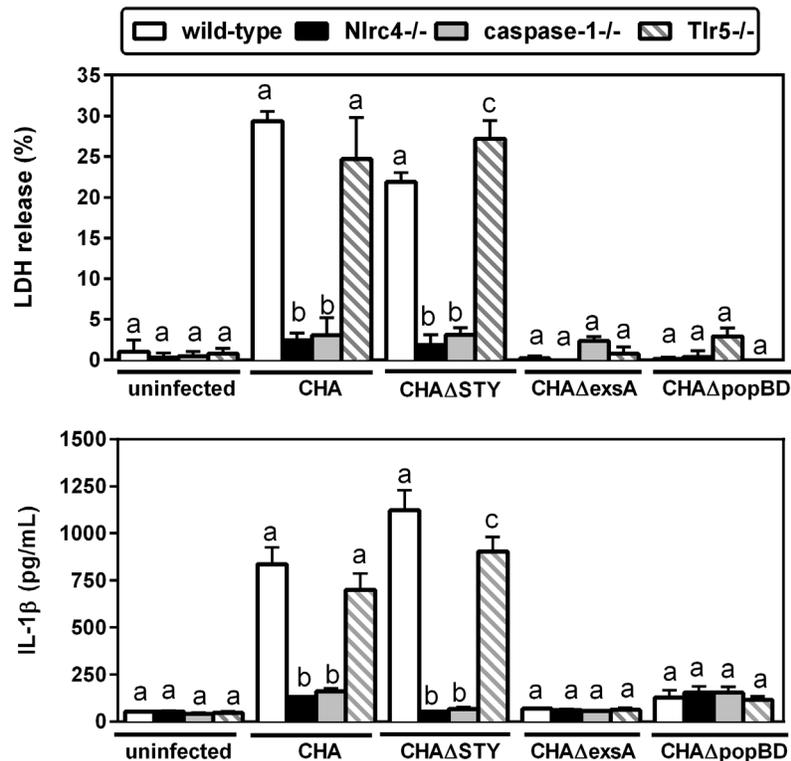Statistical analysis: r = Pearson coefficient of the correlation.

Figure S10

INP1855 inhibits YscN ATPase activity

Inhibition of purified YscN T3SS ATPase by INP1855. His-YscN (25 mg/L) was incubated for the indicated times in presence of 250 µM INP1855 (left) or with increasing concentrations of INP1855 for 1h (right). Enzyme and INP1855 were incubated for the indicated times, after which ATP (4 mM) was added to the samples for 30 min, and ATPase activity was measured as the amount of free phosphate liberated. Values are expressed as the percent inhibition of free phosphate release measured in the absence of INP1855. Experiments were performed in duplicates with individual values shown on the graph. The IC_{25} and IC_{50} values were calculated from sigmoidal dose-response functions with variable slope as determined by non-linear regression using GraphPad Prism®.

Corresponding method: To the best of our knowledge, the PscN ATPase of the T3SS of *P. aeruginosa* has not been fully purified so far in spite of numerous attempts including by expert groups (PhD thesis of C. Perdu from the team of I. Attrée, *Université de Grenoble,* France). We therefore took advantage of its high homology with the corresponding YscN enzyme in *Yersinia pseudotuberculosis*, for which a vector encoding the His-tagged enzyme was available to us (57 % identity; 72% positive substitutions with PscN by BLAST alignment). The enzyme was purified exactly as previously described *(Davis AJ, Diaz DAD, Mecsas J. A dominant-negative needle mutant blocks type III secretion of early but not late substrates in Yersinia. Mol Microbiol. 2010;76:236-259*) and its activity assessed using the MAK113 kit from Sigma-Aldrich and following the recommendations of the manufacturer.
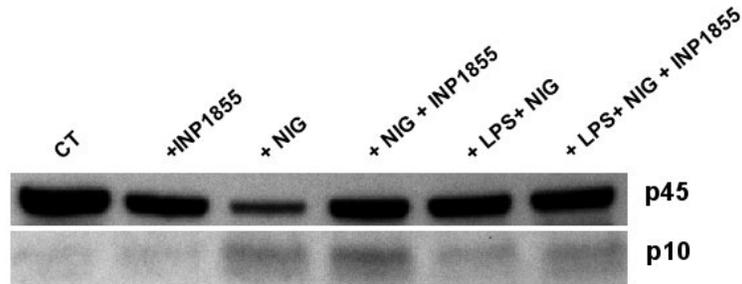
Figure S11

Cytotoxicity and IL-1β secretion induced by *P. aeruginosa* in wild-type, *Nlrc4 -/-, caspase-1 -/-, Tlr5 -/-* mouse macrophages.

Peritoneal macrophages were preincubated during 12 hours with 50 ng/mL of LPS and thereafter infected with different strains (20 bacteria/cell) of *P. aeruginosa* (CHA, CHAΔ*STY*, CHAΔ*exsA*, CHAΔ*popBD*) during 90 minutes after which LDH and IL-1β release were measured in the supernatant. Data are mean ± SD of 4 independent determinations. Statistical analyses (one-way ANOVA with Tukey's post-test for multiple comparisons among cell types for each bacterial strain): values with different letters are significantly different from each other (p<0.05).

CHA caused 25-30 % cytotoxicity and a massive release of IL-1β in wild-type and in *trl5 -/-* macrophages. Remarkably, CHAΔSTY showed a similar profile despite the fact it did not express any toxin but still the translocation apparatus. On the contrary, both strains were unable to affect *nlrc4 -/-* or in *caspase1 -/-* macrophages. On the other side, CHAΔ*exsA* and CHAΔ*popBD* did not show any toxicity, whatever the cell type used, and did not cause any significant release of IL-1β, confirming the T3SS apparatus role in inflammasome activation. Thus, taken together, these data confirm that strains expressing a functional T3SS apparatus can induce IL-1β release and cytotoxicity that require the expression of NLRC4 and caspase-1.

Method for cell collection: peritoneal macrophages were collected from mice (C57bl6/J background), using in parallel wild-type and knock-out mice nlrc4-/- (provided by Dr Mathias Chamaillard, Institut Pasteur, Lille, France), tlr5-/- (provided by Dr Michel Chignard; Institut Pasteur, Paris, France) and caspase-1-/- (The Jackson Laboratory, Bar Harbor, ME) [*Faure E, Mear JB, Faure K, Normand S, Couturier-Maillard A et al. Pseudomonas aeruginosa type-3 secretion system dampens host defense by exploiting the NLRC4-coupled inflammasome. Am J Respir Crit Care Med. 2014;189:799-811*]. Mice received an injection of 4% thioglycolate (Sigma-Aldrich, St Louis, MO) 5 days before collection of cells. Peritoneal macrophages were cultured in IMDM medium supplemented with 10% fetal calf serum, 100 U/ml penicillin, and 100 mg/L streptomycin (GIBCO, Life technologies, Carlsbad, CA) in a 5% CO_2 atmosphere at 37°C.
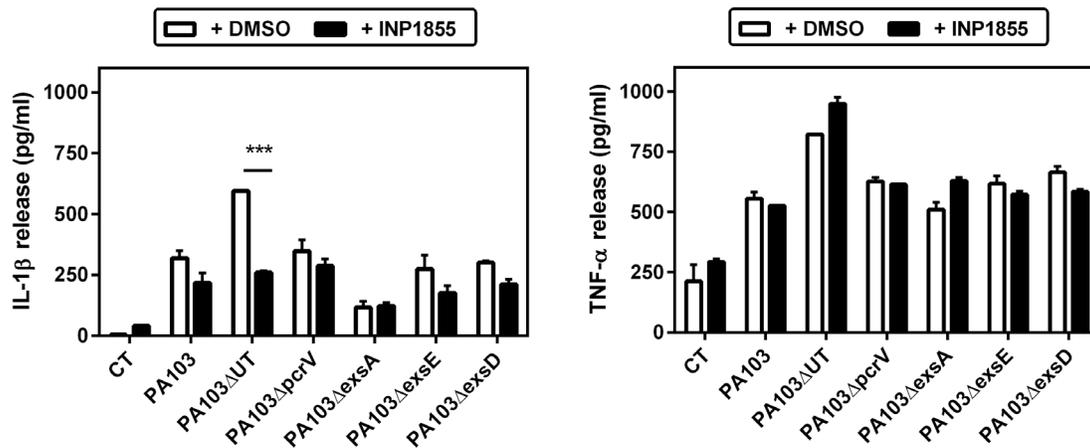
Figure S12

INP1855 does not inhibit caspase-1 activation

Cells were incubated during 5h in the presence of 60 µM of INP1855 in 0.6 % DMSO or the corresponding vehicle (control), 0.02 µM nigericin (NIG), 100 ng/mL LPS or the indicated combinations. 30 µg of total cell lysates were separated by SDS-PAGE and analyzed by western blotting for the presence of uncleaved pro- (45 kDa) and biologically active cleaved form (10 KDa) of caspase-1.
The figure shows a representative gel out of 2 experiments.

No change in caspase-1 activation induced by nigericin alone or combined with LPS was

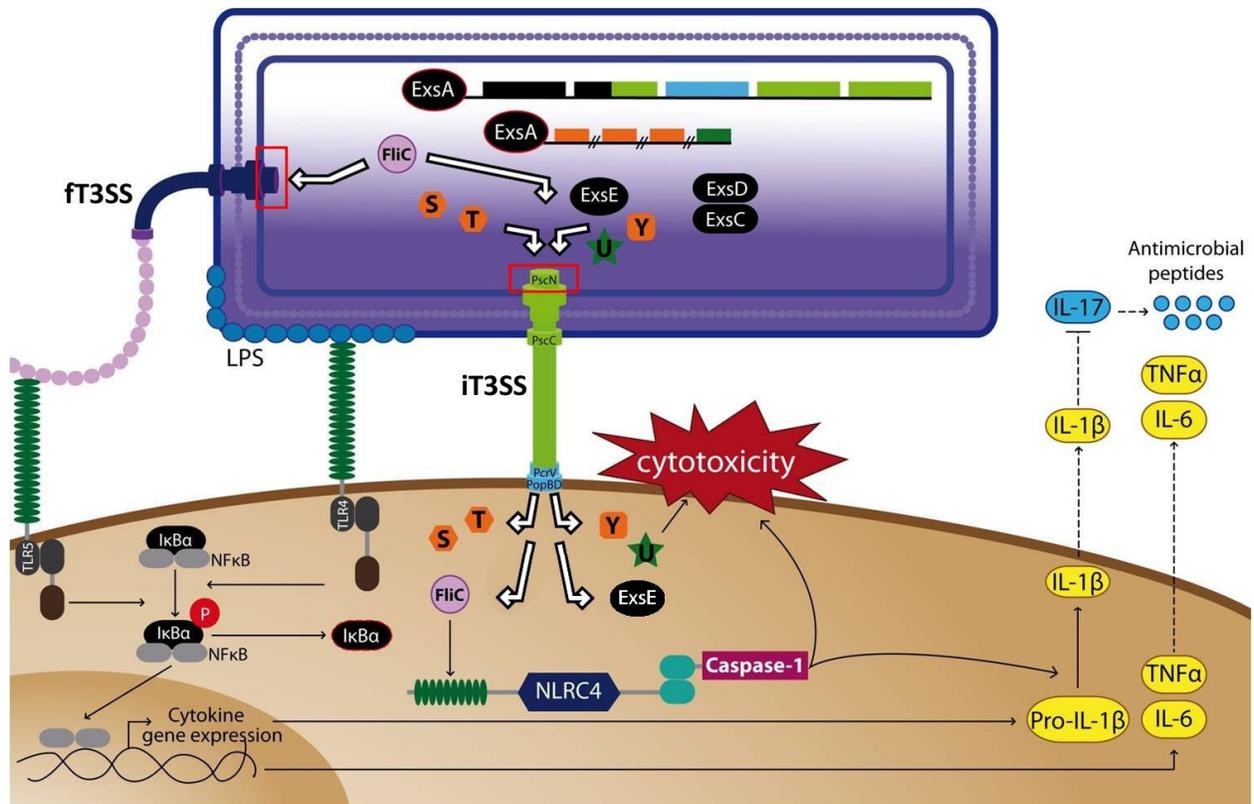noticed in cells co-incubated in the presence of the inhibitor.

Figure S13

INP1855 decreases IL-1β secretion induced by a iT3SS-positive strain that does not express ExoU, without affecting TNF-α secretion.

Influence of INP1855 on cytokine secretion from THP-1 monocytes were pre-incubated during 4h in the presence of LPS (100 ng/mL) and Brefeldin A (10 mg/L), after which cells were centrifuged, washed and incubated during 5h with different bacterial strains (10 bacteria/cell) in the presence of 60 µM INP1855 in 0.6% DMSO or in 0.6% DMSO (control). IL-1β (left) and TNF-α (right) were then measured in the supernatant. All values are the mean ± SEM (n=2). Statistical analysis: *** $p<0.001$ (two-way ANOVA, Bonferroni post-test) comparing control conditions with INP1855.

IL-1β release induced by PA103 and its mutants was low, except for PA103Δ*UT* (the only one activating NLRC4 inflammasome). This could be due either to the high cytotoxicity of the ExoU toxin which kills the cells (see **Fig. 3**) before inflammasome activation takes place or to the fact that ExoU itself has been described as an inhibitor of inflammasome activation [*Sutterwala FS, Mijares LA, Li L, Ogura Y, Kazmierczak BI, Flavell RA. Immune recognition of Pseudomonas aeruginosa mediated by the IPAF/NLRC4 inflammasome. J Exp Med. 2007;204:3235-3245].* For the PA103Δ*UT* mutant, INP1855 brought IL-1β levels back to the value observed with PA103. As also described for CHA and its mutants, no effect of INP1855 was observed on TNF-α release.

Figure S14

Pictorial view of the model of action of INP1855

The bacterium is represented in violet at the top of the figure; the eukaryotic cell (focusing on a cell expressing the NLRC-4 inflammasome), in brown on the bottom.

In control conditions (no inhibitor), iT3SS (injectisome) can inject several proteins into the host cell cytosol (see white arrows pointing to secretion/translocation), among which the exoenzymes S, T, Y or U toxins, the negative regulator ExsE, and the FliC protein (monomeric subunit of flagellum). The latter can activate the NLRC4 inflammasome, causing caspase-1 activation. The active enzyme cleaves pro-IL-1β to IL-1β (as well as pro-IL-18 to IL-18; not shown), which are released out of the cell and inhibit IL-17 signaling. LPS or fT3SS (flagellum) can activate the NFκB pathway via TLR4 or TLR5 signaling via phosphorylation of IκBα. In the presence of INP1855, secretion of proteins by iT3SS (including toxins and FliC) and flagellar motility are impaired, probably due to an inhibition of the ATPase of the basal core of these systems which share high structural and functional homology. Caspase-1 activation and subsequent IL-1β release are inhibited, presumably because iT3SS inhibition prevents the delivery into the host cells of proteins recognized by NAIP (Neuronal Apoptosis Inhibitory Proteins) and activating NLRC4 inflammasome, like FliC (note that other NAIP ligands have been described, like iT3SS inner rod proteins [in murine cells] or needle proteins [in both human and murine cells]).
Putative targets for INP1855 are highlighted by a red rectangle.